MODELING OF LOW-CONTRAST PHOTONIC CRYSTALS WITH COUPLED-MODE EQUATIONS

By

Dmitri Agueev

SUBMITTED IN PARTIAL FULFILLMENT OF THE
REQUIREMENTS FOR THE DEGREE OF
MASTER OF SCIENCE
AT
MCMASTER UNIVERSITY
HAMILTON, ONTARIO
SEPTEMBER 2004

MCMASTER UNIVERSITY

DEGREE:	Master of Science, 2004
DEPARTMENT:	Mathematics and Statistics, Hamilton, Ontario
UNIVERSITY:	McMaster University
TITLE:	Modeling of low-contrast photonic crystals with coupled-mode equations
AUTHOR:	Dmitri Agueev
SUPERVISOR:	Dmitry Pelinovsky
PAGES:	viii,81

MCMASTER UNIVERSITY
DEPARTMENT OF
MATHEMATICS AND STATISTICS

The undersigned hereby certify that they have read and recommend to the Faculty of Graduate Studies for acceptance a project entitled "**Modeling of low-contrast photonic crystals with coupled-mode equations**" by **Dmitri Agueev** in partial fulfillment of the requirements for the degree of **Master of Science**.

Dated: September 2004

Supervisor: _____
Dmitry Pelinovsky

Readers: _____
Walter Craig

_____
Matheus Grasselli

To my parents

Table of Contents

Abstract

We show that the coupled-mode equations can be used for analysis of resonant interaction of Bloch waves in low-contrast cubic-lattice photonic crystals. Coupled-mode equations are derived from Maxwell's equations using asymptotic methods.

We prove the existence and uniqueness theorem for a solution of the boundary value problem for transmission of N resonant waves in convex domain (linear and non-linear cases).

The analytical solutions for linear boundary-value problem for the stationary transmission of four counter-propagating and two oblique waves on the plane are found by using separation of variables and generalized Fourier series. We give an alternative proof that the linear stationary boundary-value problem for four counter-propagating and two oblique waves on the plane is well-posed. For applications in photonic optics, we compute integral invariants for the transmission, reflection and diffraction of resonant waves.

We recast the problem for four counter-propagating waves on the plane in a multi-symplectic Hamiltonian viewpoint, which gives further insights into the problem.

Acknowledgments

I am happy to take this opportunity to express my gratitude to Dr. Dmitry Pelinovsky for introducing me to the subject with so many wonderful symmetries and Dr. Walter Craig for his break-through discussions on infinite-dimensional hamiltonian systems. Special thanks to my supervisor Dmitry Pelinovsky for his help and patience. I look forward to working together in the future.

As regards the preparation of the theses, I thank Filip Machi, Jerrold Marsden and Wendy McKay for creating "FasTeX" – the program that proved to be very useful and linguistically amusing.

Most of all I ought to thank my friend Ramy Gohary whose support and interest in my work kept me going.

This research was supported by my supervisor and the Department of Mathematics at McMaster University.

Chapter 1

Introduction

Photonic crystals have attracted much attention in recent years. These crystals serve as conducting media for electromagnetic waves. They are expected to exhibit properties similar to those of solid crystals as conducting media in the case of electromagnetic and electronic waves.

It is well known from the quantum theory of solids that the energy spectrum of an electron in a solid consists of bands separated by gaps (see for instance, [Ki]). This band-gap structure arises due to periodicity of the underlying crystal, and is common for many periodic differential operators (see the so-called Floquet-Bloch theory in [E], [K1], [RS]). The basic mathematical theory that describes how the band gaps arise in periodic dielectric and acoustic media was essentially constructed in [FK1], [FK2], [K2] using Floquet-Bloch theory. It was shown that high-contrast photonic crystals may exhibit band gaps for some configuration of the refractive index $n(\mathbf{x})$ and no band gaps exist for low-contrast photonic crystals, however stop bands may occur [K1], [K2].

The basic physical reason for the rise of gaps lies in the coherent multiple scattering and interference of waves inside the crystal – the Bragg resonance of the waves with

the crystal structure. The tremendous number of applications that are expected in optics and electronics (including high-efficiency lasers, laser diodes, etc.) warrants thorough investigation of this matter (see for instance, [JMW]). Thus, one is not surprised by the persistent attention that this problem has attracted.

There is an obvious similarity between photonic crystal and non-homogeneous acoustic media (acoustically modulated media) – both can be viewed as a continuous periodic distribution of "reflectors" to the opposite of well-defined discrete planes of the solid crystal, which makes the development of the theory of photonic crystals even more important and ground it on the works on light scattering of Brillouin (who followed up some work that had been begun earlier by Einstein) and Rayleigh (an excellent book on acousto-optics with historical overview is [Ko]). In fact the idea of a coupled-mode approach in modeling of photonic crystals seems to come from acousto-optics (Raman-Nath equations in acousto-optics). One of the latest cross-infiltrations uses Feynman diagram techniques, or path integrals in modeling multi-scattered light ([Ko], [S]). The beauty of Feynman diagrams lies in the fact that certain path integrals may be ignored because physical reasoning tells us that their contribution is negligible.

The purpose of this thesis is to apply coupled-mode equations for analysis and modeling of resonant interaction of Bloch waves in low-contrast cubic lattice photonic crystal. Modeling of time-dependent responses of photonic crystals in three spatial dimensions can be computationally difficult in the framework of the Maxwell equations, especially if the nonlinear and nonlocal dispersive terms are taken into account. A more efficient method is based on reduction of Maxwell equations to the coupled-mode equations [SS]. For instance, shock wave singularities may occur in the

nonlinear Maxwell equations but they do not occur in the nonlinear coupled-mode equations [GWH]. Coupled-mode equations are typically derived in the first band gap of the Bragg resonance between two counter-propagating waves in one spatial dimension [SS1, SS2]. More complicated coupled-mode equations are recently considered for three-dimensional nonlinear photonic crystals [AJ1, AJ2, AS, BS]. Recent reviews [BF1, BF2] include also classification of different resonances of Bloch waves in photonic crystals with quadratic nonlinearities.

In the thesis

- We classify wave resonances and coupled-mode equations for low-contrast cubic-lattice photonic crystals in three spatial dimensions. Since low-contrast crystals do not support band gaps beyond one dimension [K1, K2], resonances are considered in stop bands of the linear spectrum [Ki]. Stop bands occur between resonant counter-propagating waves, which could be coupled with other oblique Bloch waves. The number of resonant Bloch waves depends on the geometric configuration of the incident wave with respect to the cubic lattice.

- We derive coupled mode equations by using perturbation series expansions of Maxwell's equations. We study coupled mode equations in bounded domains, subject to radiation boundary conditions. Such boundary conditions describe the transmission of incident Bloch waves, which generate resonantly reflected and diffracted Bloch waves in the photonic crystals.

- We generalize the coupled-mode equations to include the weakly nonlinear (cubic) terms and to extend the time-dependent problems to the nonlinear coupled-mode equations [SGS, Sh].

- We prove an existence and uniqueness theorem for a solution of N-wave coupled-mode boundary value problem (linear and non-linear cases) using a contraction mapping argument.

- We obtain the analytic solution for the linear coupled-mode equations for four counter-propagating and two oblique Bloch waves on the plane. We give an alternative proof of well-posedness of the linear stationary problem We prove the well-posedness of the linear stationary problem by using separation of variables and generalized Fourier series [St]. Eigenfunction expansions and convergence of generalized Fourier series follow from the general theory [CL]. As a result, we construct explicit analytical expressions for stationary transmission, reflection, and diffraction of resonant Bloch waves, which are used in modeling of the low-contrast photonic crystals.

- We recast the problem for four counter-propagating waves on the plane from multi-symplectic Hamiltonian viewpoint, which gives further insights into the problem.

The main contributions of the thesis to the subject are

- The existence and uniqueness theorems for a solution of N-wave coupled-mode boundary value problem (linear and non-linear cases).

- Construction of analytical solutions for four counter-propagating and two oblique Bloch waves on the plane.

This thesis is partly based on the work [AP] of Dmitry Pelinovsky and myself.
Everywhere in this thesis we are using Einstein's summation rule – summation over repeating indexes.

Chapter 2

Resonances of electromagnetic waves in photonic crystals

2.1 Maxwell equation for light propagation in photonic crystals

Propagation of electromagnetic waves in dielectrics is governed by Maxwell's equations [LL1], which

$$\nabla \cdot \mathbf{D} = 0 \quad , \quad \nabla \cdot \mathbf{B} = 0,$$
$$\nabla \times \mathbf{E} = -\frac{1}{c}\frac{\partial \mathbf{B}}{\partial t} \quad , \quad \nabla \times \mathbf{H} = \frac{1}{c}\frac{\partial \mathbf{D}}{\partial t};$$

where $\mathbf{E}$ and $\mathbf{H}$ are electric and magnetic field vectors respectively, and $\mathbf{D}$ and $\mathbf{B}$ are corresponding electric and magnetic flux densities, $\mathbf{x} = (x, y, z)$ is the physical space, t is the time variable, $\nabla = (\partial_x, \partial_y, \partial_z)$ is the gradient vector, and c is the speed of light. This system isn't complete unless we specify the relation between $\mathbf{D}$ and $\mathbf{E}$, as well as $\mathbf{B}$ and $\mathbf{H}$. The relation between $\mathbf{D}$ and $\mathbf{E}$ is given by the linear law [LL2]

$$D_k = \epsilon_k^s E_s,$$

where $\{\epsilon_k^s(\mathbf{x})\}$ is the dielectric permittivity tensor. It is usually assumed that $\mathbf{B} = \mu\mathbf{H} = \mathbf{H}$ (which is to say that polarization effects are much stronger then magnetic).

If the medium is isotropic, then $\epsilon_k^s = \epsilon\delta_k^s$, where ϵ – is a scalar and δ_k^s is a Kroneker symbol, i.e in the simplest of cases the permittivity is determined by a single scalar. In the general case the permittivity $\{\epsilon_k^s\}$ will be more complicated. We consider a cubic crystal as the medium represented by the cubic lattice in $\mathbb{R}^3$ as depicted in Figure 2.1.

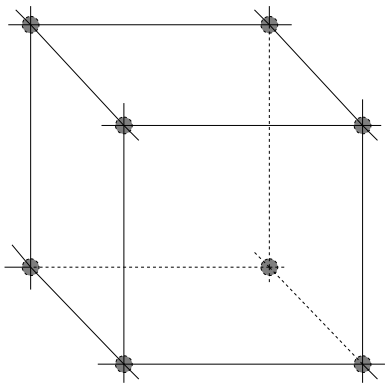

Figure 2.1: Cubic lattice R in $\mathbb{R}^3$.

The crystal is assumed to be ideal with the lattice R that fills the whole space. It is clear that the group of symmetry of this crystal $S_3(R)$ contains, in particular, the following orthogonal transformations:

$$\alpha_1 = \begin{pmatrix} 0 & 1 & 0 \\ -1 & 0 & 0 \\ 0 & 0 & 1 \end{pmatrix}; \alpha_2 = \begin{pmatrix} 0 & 0 & 1 \\ 0 & 1 & 0 \\ -1 & 0 & 0 \end{pmatrix}; \alpha_3 = \begin{pmatrix} 1 & 0 & 0 \\ 0 & 0 & 1 \\ 0 & -1 & 0 \end{pmatrix},$$

i.e. α_1 – is the rotation on $\frac{\pi}{2}$ about the z-axis, α_2 – is the rotation on $\frac{\pi}{2}$ about the y-axis,α_3 – is the rotation on $\frac{\pi}{2}$ about the x-axis.

Since these three rotations preserve the lattice R, the tensor $\{\epsilon_k^s\}$ is invariant under those symmetry operations. Writing it in analytical form, we denote $\{\epsilon_k^s\}$ as the matrix A; then $A_i' = \alpha_i A \alpha_i^{-1} = A$ for any $i = 1, 2, 3$. Computing the matrix A_i' we

have

$$A_1' = \begin{pmatrix} \epsilon_2^2 & -\epsilon_1^2 & \epsilon_3^2 \\ -\epsilon_2^1 & \epsilon_1^1 & -\epsilon_3^1 \\ \epsilon_2^3 & -\epsilon_1^3 & \epsilon_3^3 \end{pmatrix} = \begin{pmatrix} \epsilon_1^1 & \epsilon_2^1 & \epsilon_3^1 \\ \epsilon_1^2 & \epsilon_2^2 & \epsilon_3^2 \\ \epsilon_1^3 & \epsilon_2^3 & \epsilon_3^3 \end{pmatrix} = A.$$

It follows that $\epsilon_1^1 = \epsilon_2^2$; in the same manner computing matrices A_2' and A_3', we get $\epsilon_1^1 = \epsilon_2^2 = \epsilon_3^3$. The group $S_3(R)$ contains three more transformations:

$$\beta_1 = \begin{pmatrix} -1 & 0 & 0 \\ 0 & -1 & 0 \\ 0 & 0 & 1 \end{pmatrix}; \beta_2 = \begin{pmatrix} -1 & 0 & 0 \\ 0 & 1 & 0 \\ 0 & 0 & -1 \end{pmatrix}; \beta_3 = \begin{pmatrix} 1 & 0 & 0 \\ 0 & -1 & 0 \\ 0 & 0 & -1 \end{pmatrix},$$

i.e. $\beta_1 = \alpha_1^2$ – is the rotation on π about the z-axis, $\beta_2 = \alpha_2^2$ – is the rotation on π about the y-axis, $\beta_3 = \alpha_3^2$ – is the rotation on π about the x-axis. Again the lattice is transformed into itself, that gives us $\tilde{A}_i = \beta_i A \beta_i^{-1} = A$,for $1 \leq i \leq 3$. Computing matrix $\tilde{A}_i$ we get

$$\tilde{A}_1 = \begin{pmatrix} \epsilon_1^1 & \epsilon_2^1 & -\epsilon_3^1 \\ \epsilon_1^2 & \epsilon_2^2 & -\epsilon_3^2 \\ -\epsilon_1^3 & -\epsilon_2^3 & -\epsilon_3^3 \end{pmatrix} = \begin{pmatrix} \epsilon_1^1 & \epsilon_2^1 & \epsilon_3^1 \\ \epsilon_1^2 & \epsilon_2^2 & \epsilon_3^2 \\ \epsilon_1^3 & \epsilon_2^3 & \epsilon_3^3 \end{pmatrix} = A.$$

It follows that $\epsilon_3^1 = \epsilon_3^2 = \epsilon_1^3 = \epsilon_2^3 = 0$; computing matrices $\tilde{A}_2$ and $\tilde{A}_3$, we get $\epsilon_j^i = 0$ for $i \neq j$. Thus finally $A = \{\epsilon_k^s\} = \epsilon \begin{pmatrix} 1 & 0 & 0 \\ 0 & 1 & 0 \\ 0 & 0 & 1 \end{pmatrix}$,i.e $\epsilon_k^s = \epsilon \delta_k^s$, where ϵ is a scalar. We have shown the following: the permittivity of the cubic crystal is isotropic (does not depend on the direction as for isotropic materials). This result is not necessarily physically obvious since one might expect that for instance permittivity in the direction of the crystal edge would differ from that in the diagonal direction.

Adding the empirical material equations

$$\mathbf{D} = \epsilon \mathbf{E}$$

$$\mathbf{B} = \mu \mathbf{H}$$

to the Maxwell system we obtain:

$$\nabla \cdot \epsilon \mathbf{E} = 0 \quad , \quad \nabla \cdot \mu \mathbf{H} = 0,$$
$$\nabla \times \mathbf{E} = -\frac{1}{c}\frac{\partial \mu \mathbf{H}}{\partial t} \quad , \quad \nabla \times \mathbf{H} = \frac{1}{c}\frac{\partial \epsilon \mathbf{E}}{\partial t}$$

Usually $\mu = 1$ which corresponds to nonmagnetic medium. Eliminating $\mathbf{H}$ from this system, we have

$$\nabla \times \nabla \times \mathbf{E} = -\frac{1}{c}\frac{\partial}{\partial t}\mu \nabla \times \mathbf{H} = -\frac{1}{c^2}\frac{\partial \mu \epsilon \mathbf{E}}{\partial t}.$$

As $\nabla \times \nabla \times \mathbf{E} = \nabla(\nabla \cdot \mathbf{E}) - \triangle \mathbf{E}$, we obtain the equation on $\mathbf{E}$

$$\nabla^2 \mathbf{E} - \frac{n^2}{c^2}\frac{\partial^2 \mathbf{E}}{\partial t^2} = \nabla(\nabla \cdot \mathbf{E}),$$

where $n = \sqrt{\mu\epsilon}$. Thus, the linear periodic properties of the isotropic photonic crystals can be modelled with the Maxwell equations:

$$\nabla^2 \mathbf{E} - \frac{n^2}{c^2}\frac{\partial^2 \mathbf{E}}{\partial t^2} = \nabla\left(\nabla \cdot \mathbf{E}\right), \qquad \nabla \cdot \left(n^2 \mathbf{E}\right) = 0, \tag{2.1}$$

where $n = n(\mathbf{x})$ is the periodic refractive index.

According to Floquet-Bloch theory the linear Maxwell equations (2.1) with periodic $n(\mathbf{x})$ can be reduced to a spectral problem for the vector function

$$\mathbf{E}(\mathbf{x}, t) = \boldsymbol{\psi}(\mathbf{x}) e^{-i\omega t}$$

where ω is the eigenvalue and $\boldsymbol{\psi}(\mathbf{x})$ is the eigenvector. When $n_0(\mathbf{x})$ is a periodic function in x, y, z with periods x_0, y_0, z_0, respectively, the eigenvector $\boldsymbol{\psi}(\mathbf{x})$ has the form of a Bloch wave

$$\psi(\mathbf{x}) = \boldsymbol{\Psi}(\mathbf{x}) e^{i(k_x x + k_y y + k_z z)}$$

where $\boldsymbol{\Psi}(\mathbf{x})$ is periodic in x, y, and z with periods x_0, y_0, and z_0, and $\omega = \omega(k_x, k_y, k_z)$. No band gaps exist in the linear spectrum for low-contrast photonic crystals. As a

result, a bounded Bloch functions $\boldsymbol{\psi}(\mathbf{x})$ will exist for any value of $\omega \in \mathbb{R}$. Highly-contrast photonic crystals may however exhibit band gaps for some configurations of the linear refractive index $n^2(\mathbf{x})$ [K2].

2.2 Bragg resonance and the Brillouin construction

When the optical material is homogeneous, such that $n(\mathbf{x}) = n_0$ is constant, the linear spectrum of the Maxwell equations (2.1) is defined by the free transverse waves,

$$\mathbf{E}(\mathbf{x}, t) = \mathbf{e}_{\mathbf{k}} e^{i(\mathbf{k}\cdot\mathbf{x} - \omega t)}, \tag{2.2}$$

where $\mathbf{e}_{\mathbf{k}}$ is the polarization vector, $\mathbf{k} = (k_x, k_y, k_z)$ is the wave vector, and $\omega = \omega(\mathbf{k})$ is the wave frequency. It follows from the system (2.1) that

$$\mathbf{k} \cdot \mathbf{e}_{\mathbf{k}} = 0, \qquad \omega^2 = \frac{c^2}{n_0^2}\left(k_x^2 + k_y^2 + k_z^2\right). \tag{2.3}$$

For each wave vector $\mathbf{k}$, there exist two independent polarizations $\mathbf{e}_{\mathbf{k}}^{(1)}$ and $\mathbf{e}_{\mathbf{k}}^{(2)}$, such that $\mathbf{e}_{\mathbf{k}}^{(1)} \cdot \mathbf{e}_{\mathbf{k}}^{(2)} = 0$. This degeneracy in the polarization vector is neglected here by the assumption that the incident wave is linearly polarized.

When the optical material is periodic, such that $n(\mathbf{x} + \mathbf{x}_0) = n(\mathbf{x}_0)$, the linear spectrum of the Maxwell equations (2.1) is defined by the Bloch waves:

$$\mathbf{E}(\mathbf{x}, t) = \boldsymbol{\Psi}(\mathbf{x}) e^{i(\mathbf{k}\cdot\mathbf{x} - \omega t)}, \tag{2.4}$$

where $\boldsymbol{\Psi}(\mathbf{x} + \mathbf{x}_0) = \boldsymbol{\Psi}(\mathbf{x})$ is the periodic envelope, $\mathbf{k} = (k_x, k_y, k_z)$ is the wave vector, and $\omega = \omega(\mathbf{k})$ is the wave frequency.

The geometric configuration of the photonic crystal is defined by the fundamental (linearly independent) lattice vectors $\mathbf{x}_{1,2,3}$ and fundamental reciprocal lattice vectors

$\mathbf{k}_{1,2,3}$, such that $\mathbf{k}_i \cdot \mathbf{x}_j = 2\pi\delta_{i,j}$, where $1 \leq i, j \leq 3$ [Ki]. Therefore, the basis $\mathbf{k}_{1,2,3}$ is dual to the basis $\mathbf{x}_{1,2,3}$ and the linear refractive index $n(\mathbf{x})$ can be expanded into triple Fourier series:

$$n(\mathbf{x}) = n_0 \sum_{(n,m,l)\in\mathbb{Z}^3} \alpha_{n,m,l} e^{i(n\mathbf{k}_1 + m\mathbf{k}_2 + l\mathbf{k}_3)\cdot\mathbf{x}} = n_0 \sum_{\mathbf{G}} \alpha_{\mathbf{G}} e^{i\mathbf{G}\mathbf{x}} \tag{2.5}$$

where $\mathbf{G}$ is the vector in dual basis $\mathbf{G} = n\mathbf{k}_1 + m\mathbf{k}_2 + l\mathbf{k}_3, (n, m, l) \in \mathbb{Z}^3$ and the factor n_0 is included for convenience. If n_0 is the mean value of $n(\mathbf{x})$, then $\alpha_{0,0,0} = 1$.

Let the wave vector $\mathbf{k}$ in the incident Bloch wave (2.4) be fixed $\mathbf{k} = \mathbf{k}_{\text{in}}$. The incident wave vector $\mathbf{k}_{\text{in}}$ is expanded in terms of the lattice vectors:

$$\mathbf{k}_{\text{in}} = \frac{1}{2}\left(p\mathbf{k}_1 + q\mathbf{k}_2 + r\mathbf{k}_3\right),$$

where $(p, q, r) \in \mathbb{R}^3$ and the factor $\frac{1}{2}$ is introduced for convenience. The Bloch wave (2.4) is represented by triple Fourier series for $\mathbf{\Psi}(\mathbf{x})$, such that $\mathbf{E}(\mathbf{x}, t)$ consists of an infinite superposition of free transverse waves with the wave vectors $\mathbf{k}' = \mathbf{k}_{\text{out}}^{(n,m,l)}$:

$$\begin{aligned} \mathbf{k}' &= \mathbf{k} + \mathbf{G} \\ \mathbf{k}_{\text{out}}^{(n,m,l)} &= \mathbf{k}_{\text{in}} + n\mathbf{k}_1 + m\mathbf{k}_2 + l\mathbf{k}_3, \qquad (n, m, l) \in \mathbb{Z}^3. \end{aligned} \tag{2.6}$$

As the scattering of light is considered to be elastic, we introduce the following energy and momentum constraint on the resonating waves

Definition 2.1 *The wave vector* $\mathbf{k}_{\text{out}}^{(n,m,l)}$ *with a non-empty triple* (n, m, l) *is said to be* resonant *with the wave vector* $\mathbf{k}_{\text{in}}$*, if* $|\mathbf{k}_{\text{out}}^{(n,m,l)}| = |\mathbf{k}_{\text{in}}|$*, such that* $|\omega(\mathbf{k}_{\text{out}}^{(n,m,l)})| = |\omega(\mathbf{k}_{\text{in}})|$.

The resonance conditions are illustrated in Figure 2.2.

From our result $\Delta\mathbf{k} = \mathbf{G}$, the resonance condition is $(\mathbf{k} + \mathbf{G})^2 = k^2$, or

$$2\mathbf{k} \cdot \mathbf{G} + G^2 = 0 \tag{2.7}$$

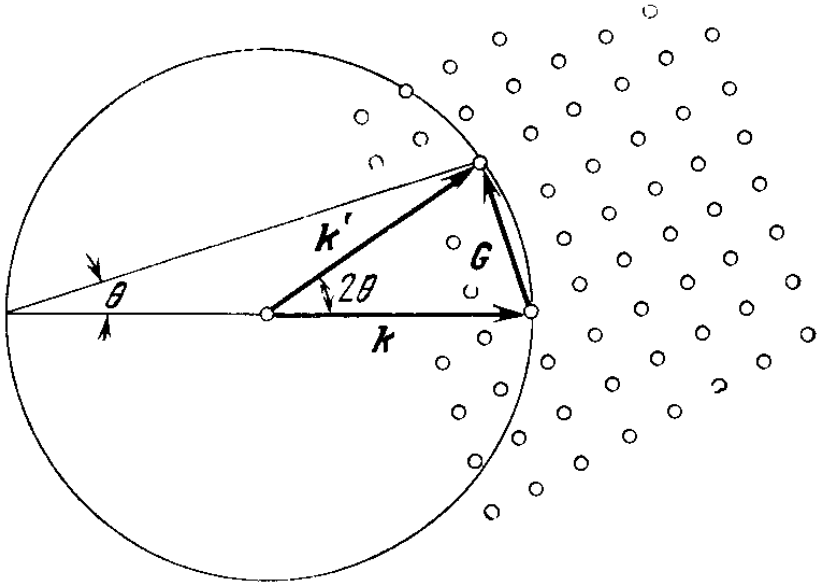

Figure 2.2: The points on the right of the sphere are reciprocal lattice points of the crystal. The vector $\mathbf{k}$ is drawn in the direction of the incident beam and it terminates at any reciprocal lattice point. We draw a sphere of radius k about the origin of $\mathbf{k}$. A diffracted beam will be formed if this sphere intersects any other point in the reciprocal lattice. The sphere as drawn intersects a point connected with the end of $\mathbf{k}$ by reciprocal lattice vector $\mathbf{G}$. The diffracted beam is in the direction $\mathbf{k}' = \mathbf{k} + \mathbf{G}$. This construction is due to P.P. Ewald. The figure is taken from [Ki]

This is the central result in the theory of elastic scattering in a periodic lattice. The identical result occur in the theory of the electron energy band structure of crystals [Ki]. Notice that if $\mathbf{G}$ is a reciprocal lattice vector, $-\mathbf{G}$ is also one; thus we can equally well write (2.7) as $2\mathbf{k} \cdot \mathbf{G} = G^2$.

The Brillouin zone gives a vivid geometrical interpretation of the resonance condition $2\mathbf{k} \cdot \mathbf{G} = G^2$ or

$$\mathbf{k} \cdot (\frac{1}{2}\mathbf{G}) = (\frac{1}{2}G)^2 \tag{2.8}$$

See the Figure 2.3.

We construct a plane normal to the vector $\mathbf{G}$ at the midpoint; any vector $\mathbf{k}$ from the origin to the plane will satisfy the resonance condition. The plane thus described forms a part of the zone boundary. An incident wave on the crystal will be diffracted if it's wavevector has the magnitude and direction required by (2.8), and the diffracted wave will be in the direction of the vector $\mathbf{k} - \mathbf{G}$.

The set of planes that are the perpendicular bisectors of the reciprocal lattice vectors are of particular importance in the theory of the wave propagation in crystals, because a wave whose wavevector drawn from the origin terminates on any of these planes will satisfy the condition for diffraction. These planes divide the Fourier space of the crystal into bits and pieces, as shown on the Figure 2.4. The central square is a primitive cell of the reciprocal lattice. It is called the first Brillouin zone. The first Brillouin zone of the cubic lattice in two dimensions is shown on the Figure 2.4. The Brillouin construction exhibits all the incident wavevectors which can be Bragg-reflected by the crystal. As can be seen from the picture there can be several resonances for one wave.

We prove a simple lemma that we will need later.

Lemma 2.2 *The number of waves resonant to the incident* $\mathbf{k}_{\text{in}}$ *is less then the number of nodes of the reciprocal lattice* $\mathbf{G}$ *lying inside the sphere of the radius* $2|\mathbf{k}_{\text{in}}|$ *centered at the origin.*

Proof. The proof is obvious from the geometrical picture, as the longest vector $\mathbf{G}$ that gives resonance is in the direction of $\mathbf{k}_{\text{in}}$. ■

We consider here a simple cubic crystal, where the fundamental lattice vectors and reciprocal lattice vectors are all orthogonal [Ki]:

$$\mathbf{x}_{1,2,3} = a\mathbf{e}_{1,2,3}, \qquad \mathbf{k}_{1,2,3} = k_0\mathbf{e}_{1,2,3}, \qquad k_0 = \frac{2\pi}{a},$$

where $\mathbf{e}_{1,2,3}$ are unit vectors in $\mathbb{R}^3$. The coordinate axes (x, y, z) are oriented along the axes of the simple cubic crystal. The set of resonant Bloch waves is given by the set of triples:

$$\mathcal{S} = \left\{ (n,m,l) \in \mathbb{Z}^3 : \ \left(n+\frac{p}{2}\right)^2 + \left(m+\frac{q}{2}\right)^2 + \left(l+\frac{r}{2}\right)^2 = \left(\frac{p}{2}\right)^2 + \left(\frac{q}{2}\right)^2 + \left(\frac{r}{2}\right)^2 \right\}, \tag{2.9}$$

or

$$\mathcal{S} = \{ (n,m,l) \in \mathbb{Z}^3 : \ n(n+p) + m(m+q) + l(l+r) = 0 \}, \tag{2.10}$$

The set $\mathcal{S}$ always has a zero solution: $(n, m, l) = (0, 0, 0)$. When $(p, q, r) \in \mathbb{Z}^3$ and $|p|+|q|+|r| \neq 0$, the set $\mathcal{S}$ has at least one non-zero solution: $(n, m, l) = (-p, -q, -r)$.

2.3 Classification of resonances

The classification of resonances can be based on geometric construction (Figure 2.4) and algebraic equation (2.9). When $(p, q, r) \in \mathbb{Z}^3$, resonant triples (n, m, l) can be all classified analytically. However, when $(p, q, r) \notin \mathbb{Z}^3$, additional resonant triples may also exist. Here we review particular resonant sets $\mathcal{S}$ for integer and non-integer values of (p, q, r).

We introduce spherical angles (θ, φ) such that the incident wave vector $\mathbf{k}_{\text{in}}$ is

$$\mathbf{k}_{\text{in}} = k\left(\sin\theta\cos\varphi, \sin\theta\sin\varphi, \cos\theta\right), \quad k \in \mathbb{R}, 0 \leq \theta \leq \pi, 0 \leq \varphi \leq 2\pi, \tag{2.11}$$

where $k = |\mathbf{k}_{\text{in}}|$. When $\theta = 0$, the wave vector $\mathbf{k}_{\text{in}}$ is perpendicular to the (x, y) crystal plane. Then

$$p = \frac{2k}{k_0}\sin\theta\cos\varphi, \quad q = \frac{2k}{k_0}\sin\theta\sin\varphi, \quad r = \frac{2k}{k_0}\cos\theta. \tag{2.12}$$

2.3.1 One-dimensional resonances of counter-propagating waves

The one-dimensional Bragg resonance occurs when the incident wave is coupled with the counter-propagating reflected wave, such that the set $\mathcal{S}$ has at least one non-zero solution: $(n, m, l) = (0, 0, -r)$, where $r \in \mathbb{Z}_+$. The values of p and q are not defined for the Bragg resonance, when $n = m = 0$. As a result, the spherical angles θ and φ in the parametrization (2.11) are arbitrary, while the wave number k satisfies the Bragg resonance condition [Ki]:

$$rk_0 = 2k\cos\theta, \tag{2.13}$$

such that $r\lambda = 2a\cos\theta$, where λ is the wavelength. The one-dimensional Bragg resonance is generalized in three dimensions for $p = q = 0$ and $r \in \mathbb{Z}_+$, when the geometric configuration for the Bragg resonance (2.13) is fixed at the specific value $\theta = 0$, and

$$\mathbf{k}_{\text{in}} = \frac{\pi}{a}(0, 0, r), \qquad \mathbf{k}_{\text{out}}^{(0,0,-r)} = \frac{\pi}{a}(0, 0, -r). \tag{2.14}$$

The incident wave is directed to the z-axis of the cubic lattice crystal and the wavelength is $\lambda = 2a/r$. The family of Bragg resonances with $p = q = 0$ and $r \in \mathbb{Z}_+$, may include not only the two counter-propagating waves (2.14) but also other Bloch waves in three-dimensional photonic crystals. The lowest-order resonant sets $\mathcal{S}$ for $p = q = 0$ and $r \in \mathbb{Z}_+$ are listed below:

$r = 1$: $\mathcal{S} = \{(0, 0, 0), (0, 0, -1)\}$

$r = 2$: $\mathcal{S} = \{(0, 0, 0), (1, 0, -1), (-1, 0, -1), (0, 1, -1), (0, -1, -1), (0, 0, -2)\}$

$r = 3$: $\mathcal{S} = \{(0, 0, 0), (1, 1, -1), (-1, 1, -1), (1, -1, -1), (-1, -1, -1), (1, 1, -2), (-1, 1, -2)\} \cup$
$\{(1, -1, -2), (-1, -1, -2), (0, 0, -3)\}$

The dimension of $\mathcal{S}$ depends on the total number of all possible integer solutions

for (n, m, l).

2.3.2 Two-dimensional resonances of counter-propagating waves

Two-dimensional Bragg resonances occur when the incident wave vector $\mathbf{k}_{\text{in}}$ is resonant to the counter-propagating reflected wave vector $\mathbf{k}_{\text{out}}^{(-p,-q,0)}$, as well as to two other diffracted wave vectors $\mathbf{k}_{\text{out}}^{(0,-q,0)}$ and $\mathbf{k}_{\text{out}}^{(-p,0,0)}$, where $(p, q) \in \mathbb{Z}_+^2$. The value of r is not defined for the two-dimensional resonance, such that the angle θ in the parametrization (2.11) is arbitrary, while k and φ satisfy the resonance conditions:

$$\varphi = \arctan\left(\frac{q}{p}\right), \qquad \sqrt{p^2+q^2}k_0 = 2k\sin\theta. \tag{2.15}$$

The two-dimensional Bragg resonances are generalized in three dimensions for $(p, q) \in \mathbb{Z}_+^2$ and $r = 0$, when the geometric configuration for the Bragg resonance (2.15) is fixed at the specific value $\theta = \frac{\pi}{2}$, and

$$\begin{aligned} \mathbf{k}_{\text{in}} &= \frac{\pi}{a}(p, q, 0), \qquad \mathbf{k}_{\text{out}}^{(-p,-q,0)} = \frac{\pi}{a}(-p, -q, 0), \\ \mathbf{k}_{\text{out}}^{(0,-q,0)} &= \frac{\pi}{a}(p, -q, 0), \qquad \mathbf{k}_{\text{out}}^{(-p,0,0)} = \frac{\pi}{a}(-p, q, 0). \end{aligned} \tag{2.16}$$

The incident wave $\mathbf{k}_{\text{in}}$ is directed along the diagonal of the (px, qy)-cell of the cubic lattice crystal and the wavelength is $\lambda = 2a/\sqrt{p^2+q^2}$.

The families of Bragg resonances with $(p, q) \in \mathbb{Z}_+^2$ and $r = 0$ may include not only the four resonant waves (2.16) but also other Bloch waves in three-dimensional photonic crystals. The lowest-order resonant sets $\mathcal{S}$ for $(p, q) \in \mathbb{Z}_+^2$ and $r = 0$ are listed below:

$p = 1, q = 1$: $\mathcal{S} = \{(0,0,0), (-1,0,0), (0,-1,0), (-1,-1,0)\}$

$p = 2, q = 1$: $\mathcal{S} = \{(0,0,0), (0,-1,0), (-1,0,1), (-1,0,-1), (-1,-1,1), (-1,-1,-1)\} \cup$
$\{(-2,0,0), (-2,-1,0)\}$

$p = 2, q = 2$: $\mathcal{S} = \{(0,0,0),(0,-1,1),(0,-1,-1),(0,-2,0),(-1,0,1),(-1,0,-1)\} \cup$
$\{(-1,-2,1),(-1,-2,-1),(-2,0,0),(-2,-1,1),(-2,-1,-1),(-2,-2,0)\}$

2.3.3 Two-dimensional resonances of oblique waves

The resonant set $\mathcal{S}$ can be non-empty for $(p,q,r) \notin \mathbb{Z}^3$, which corresponds to oblique Bloch waves. For instance, two oblique waves are resonant on the (x,y)-plane if

$$\mathbf{k}_{\rm in} = \frac{\pi}{a}(p,q,0), \qquad \mathbf{k}_{\rm out}^{(n,m,0)} = \frac{\pi}{a}(p+2n, q+2m, 0). \tag{2.17}$$

where $(n,m) \in \mathbb{Z}^2$ are arbitrary and $(p,q) \in \mathbb{R}^2$ are taken on the straight line:

$$np + mq = -(n^2+m^2). \tag{2.18}$$

Similarly, three oblique waves can be resonant on the (x,y)-plane if

$$\mathbf{k}_{\rm in} = \frac{\pi}{a}(p,q,0),\ \mathbf{k}_{\rm out}^{(n_1,m_1,0)} = \frac{\pi}{a}(p+2n_1, q+2m_1, 0),\ \mathbf{k}_{\rm out}^{(n_2,m_2,0)} = \frac{\pi}{a}(p+2n_2, q+2m_2, 0), \tag{2.19}$$

where $(n_1,m_1) \in \mathbb{Z}^2$ and $(n_2,m_2) \in \mathbb{Z}^2$ are arbitrary subject to the constraint: $m_1 n_2 \neq m_2 n_1$, while (p,q) take rational values:

$$p = \frac{m_1(n_2^2+m_2^2) - m_2(n_1^2+m_1^2)}{m_2 n_1 - m_1 n_2}, \quad q = \frac{n_1(n_2^2+m_2^2) - n_2(n_1^2+m_1^2)}{n_2 m_1 - n_1 m_2}. \tag{2.20}$$

In general case, two oblique waves (2.17) or three oblique waves (2.19) may have resonances with other Bloch waves in three-dimensional photonic crystals.

2.3.4 Three-dimensional resonances of counter-propagating waves

When $(p,q,r) \in \mathbb{Z}^3_+$, the resonant sets $\mathcal{S}$ include eight coupled waves for fully three-dimensional Bragg resonance:

$$\mathbf{k}_{\rm in} = \frac{\pi}{a}(p,q,r), \qquad \mathbf{k}_{\rm out}^{(-p,-q,-r)} = \frac{\pi}{a}(-p,-q,-r),$$

$$
\begin{aligned}
\mathbf{k}_{\text{out}}^{(-p,0,0)} &= \frac{\pi}{a}(-p,q,r), \qquad \mathbf{k}_{\text{out}}^{(0,-q,0)} = \frac{\pi}{a}(p,-q,r),\\
\mathbf{k}_{\text{out}}^{(0,0,-r)} &= \frac{\pi}{a}(p,q,-r), \qquad \mathbf{k}_{\text{out}}^{(-p,-q,0)} = \frac{\pi}{a}(-p,-q,r),\\
\mathbf{k}_{\text{out}}^{(-p,0,-r)} &= \frac{\pi}{a}(-p,q,-r), \qquad \mathbf{k}_{\text{out}}^{(0,-q,-r)} = \frac{\pi}{a}(p,-q,-r).
\end{aligned} \tag{2.21}
$$

The resonance condition for the three-dimensional Bragg resonance takes the form:

$$
\varphi = \arctan\left(\frac{q}{p}\right), \quad \theta = \arctan\left(\frac{\sqrt{p^2+q^2}}{r}\right), \quad \sqrt{p^2+q^2+r^2}k_0 = 2k, \tag{2.22}
$$

The incident wave $\mathbf{k}_{\text{in}}$ is directed along the diagonal of the (px, qy, rz)-cell of the cubic lattice crystal and the wavelength is $\lambda = 2a/\sqrt{p^2+q^2+r^2}$. The eight waves (2.21) can be coupled with some other resonant waves, such that $\dim(\mathcal{S}) \geq 8$ for $(p,q,r) \in \mathbb{Z}_+^3$. For instance, $\dim(\mathcal{S}) = 8$ for $(p,q,r) = (1,1,1)$ and $(p,q,r) = (2,1,1)$, but $\dim(\mathcal{S}) = 10$ for $(p,q,r) = (2,2,1)$ and $\dim(\mathcal{S}) = 16$ for $(p,q,r) = (3,2,1)$.

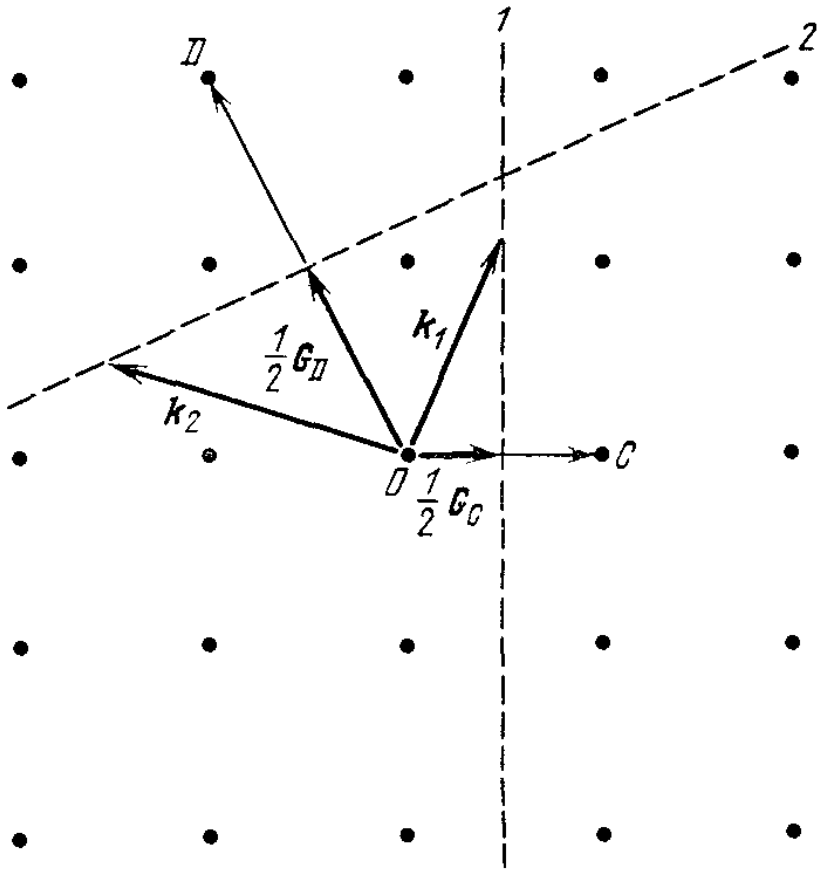

Figure 2.3: Reciprocal lattice points near the point O at the origin of the reciprocal lattice. The reciprocal lattice vector $\mathbf{G}_C$ connects points OC; and $\mathbf{G}_D$ connects OD. Two planes 1 and 2 are drawn which are perpendicular bisectors of $\mathbf{G}_C$ and $\mathbf{G}_D$, respectively. Any vector from the origin to the plane 1, such as $\mathbf{k}_1$, satisfies the diffraction condition $\mathbf{k}_1 \cdot (\frac{1}{2}\mathbf{G}_C) = (\frac{1}{2}\mathbf{G}_C)^2$. Any vector from the origin to the plane 2 , such as $\mathbf{k}_2$, satisfies the diffraction condition $\mathbf{k}_2 \cdot (\frac{1}{2}\mathbf{G}_D) = (\frac{1}{2}\mathbf{G}_D)^2$. Figure is taken from [Ki].

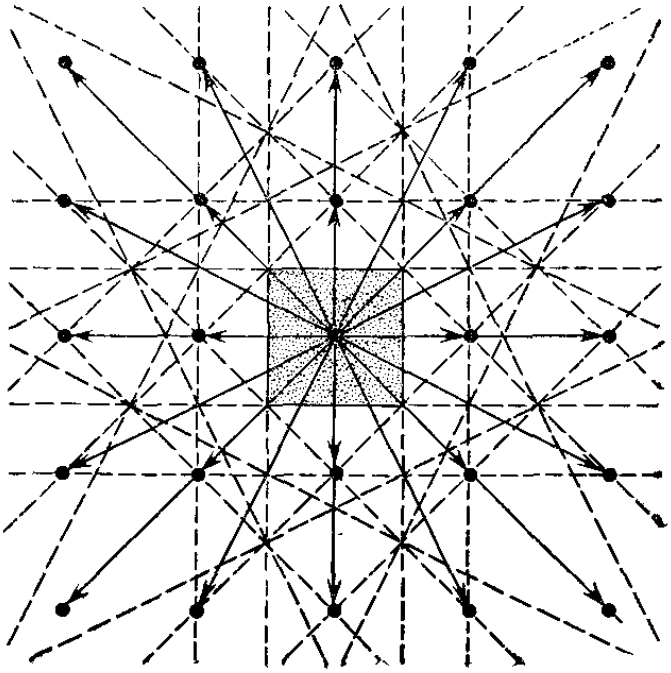

Figure 2.4: Square reciprocal lattice with reciprocal lattice vectors shown as black lines. The dashed lines are perpendicular bisectors of the reciprocal lattice vectors. The central square is the smallest volume about the origin which is bounded entirely by dashed lines. The square is the Wigner-Seitz primitive cell of the reciprocal lattice. It is called the first Brillouin zone. Figure is taken from [Ki].

Chapter 3

Derivation of coupled-mode equations

The dispersion surface $\omega = \omega(\mathbf{k})$ for the Bloch waves (2.4) in the periodic photonic crystal is defined by the profile of the refractive index $n(\mathbf{x})$. We shall consider the asymptotic approximation of the dispersion surface $\omega = \omega(\mathbf{k})$ in the limit when the photonic crystal is low-contrast, such that the refractive index $n(\mathbf{x})$ is given by

$$n(\mathbf{x}) = n_0 + \epsilon n_1(\mathbf{x}), \tag{3.1}$$

where n_0 is a constant and ϵ is small parameter. It is proved in [K1] that the Bloch waves (2.4) are smooth functions of ϵ, such that the asymptotic solution of the Maxwell equations (2.1) as $\epsilon \to 0$ takes the form of the perturbation series expansions:

$$\mathbf{E}(\mathbf{x}, t) = \mathbf{E}_0(\mathbf{x}, t) + \epsilon \mathbf{E}_1(\mathbf{x}, t) + \mathrm{O}(\epsilon^2). \tag{3.2}$$

The leading-order term $\mathbf{E}_0(\mathbf{x}, t)$ consists of free transverse waves (2.2) with wave vectors $\mathbf{k}_{\text{out}}^{(n,m,l)}$, given by (2.6), such that the asymptotic form (3.2) represents the Bloch wave (2.4) as $\epsilon \neq 0$.

Coupled-mode equations are derived by separating resonant free waves from non-resonant free waves in the Bloch wave (2.4), where the resonant set $\mathcal{S}$ with $N = \dim(\mathcal{S}) < \infty$ is defined by (2.9). Let $\mathbf{E}_0(\mathbf{x}, t)$ be a linear superposition of N resonant waves with wave vectors $\mathbf{k}_j$ at the same frequency ω:

$$\mathbf{E}_0(\mathbf{x}, t) = \sum_{j=1}^{N} A_j(\mathbf{X}, T)\mathbf{e}_{\mathbf{k}_j} e^{i(\mathbf{k}_j \mathbf{x} - \omega t)}, \qquad \mathbf{X} = \frac{\epsilon \mathbf{x}}{k}, \quad T = \frac{\epsilon t}{\omega}, \tag{3.3}$$

where ω and $\mathbf{k}_j$ are related by the same dispersion equation (2.3), $A_j(\mathbf{X}, T)$ is the envelope amplitude of the j^{th} resonant wave (2.2) and $(\mathbf{X}, T)$ are slow variables. The slow variables represent a deformation of the dispersion surface $\omega = \omega(\mathbf{k}_j)$ for free waves (2.3) due to the low-contrast periodic photonic crystal. The degeneracy in the polarization vector is neglected by the assumption that the incident wave is linearly polarized with the polarization vector $\mathbf{e}_{\text{in}} = \mathbf{e}_{\mathbf{k}_{\text{in}}}$. The triple Fourier series (2.5) for the cubic-lattice crystal is simplified as follows:

$$n_1(\mathbf{x}) = n_0 \sum_{(n,m,l) \in \mathbb{Z}^3} \alpha_{n,m,l} e^{ik_0(nx+my+lz)}, \tag{3.4}$$

where $\alpha_{0,0,0} = 0$. The Fourier coefficients $\alpha_{n,m,l}$ satisfy the constraints:

$$\alpha_{n,m,l} = \bar{\alpha}_{-n,-m,-l},$$

due to the reality of $n_1(\mathbf{x})$,

$$\alpha_{n,m,l} = \alpha_{m,n,l} = \alpha_{n,l,m} = \alpha_{l,m,n},$$

due to the crystal isotropy in the directions of x,y,z-axes, and

$$\alpha_{-n,m,l} = \alpha_{n,m,l}, \quad \alpha_{n,-m,l} = \alpha_{n,m,l}, \quad \alpha_{n,m,-l} = \alpha_{n,m,l},$$

due to the crystal symmetry with respect to the origin $(0, 0, 0)$ (the latter property can be achieved by a simple shift of (x, y, z)). It follows that all coefficients $\alpha_{n,m,l}$ for $(n, m, l) \in \mathbb{Z}^3$ are real-valued.

It follows from (2.1), (3.1), and (3.2) that the first-order correction term $\mathbf{E}_1(\mathbf{x},t)$ solves the non-homogeneous linear problem:

$$\nabla^2\mathbf{E}_1 - \frac{n_0^2}{c^2}\frac{\partial^2\mathbf{E}_1}{\partial t^2} = 2\frac{n_0^2\omega}{c^2}\frac{\partial^2\mathbf{E}_0}{\partial T\partial t} - 2k\left(\nabla\cdot\nabla_X\right)\mathbf{E}_0 + \frac{2n_0n_1(\mathbf{x})}{c^2}\frac{\partial^2\mathbf{E}_0}{\partial t^2} + \frac{2}{n_0}\nabla\left(\nabla n_1\cdot\mathbf{E}_0\right), \tag{3.5}$$

where $\nabla_X = (\partial_X, \partial_Y, \partial_Z)$ and the second equation (2.1) has been used. The right-hand-side of the non-homogeneous equation (3.5) has resonant terms, which are parallel to the free-wave resonant solutions of the homogeneous problem. The resonant terms lead to the secular growth of $\mathbf{E}_1(\mathbf{x},t)$ in t, unless they are identically zero. The latter conditions define the coupled-mode equations for amplitudes $A_j(\mathbf{X},T)$, $j = 1, ..., N$ in the general form:

$$2ik^2\left(\frac{\partial A_j}{\partial T} + \left(\frac{\mathbf{k}_j}{k}\cdot\nabla_X\right)A_j\right) + \sum_{k\neq j} a_{j,k}A_k = 0, \qquad j = 1, ..., N, \tag{3.6}$$

where the elements $\{a_{j,k}\}_{1\leq j,k\leq N}$ are related to the Fourier coefficients $\{\alpha_{n,m,l}\}_{(n,m,l)\in\mathbb{Z}^3}$ at the resonant terms $(n,m,l)\in\mathcal{S}$.

The explicit forms of the coupled-mode equations (3.6) are derived below for a number of examples of Bloch waves resonances.

3.1 Coupled-mode equations for one-dimensional resonance

The lowest-order Bragg resonance for two counter-propagating waves (2.14) occurs for $r = 1$, when

$$\mathbf{k}_1 = \frac{\pi}{a}(0,0,1), \qquad \mathbf{k}_2 = \frac{\pi}{a}(0,0,-1). \tag{3.7}$$

Let $A_1 = A_+(Z,T)$ and $A_2 = A_-(Z,T)$ be the amplitudes of the right (forward) and left (backward) propagating waves, respectively. The envelope amplitudes are not

modulated across the (X, Y)-plane, since the coupled-mode equations for $A_\pm$ are essentially one-dimensional. The polarization vectors are chosen in the x-direction, such that $\mathbf{e}_{\mathbf{k}_1} = \mathbf{e}_{\mathbf{k}_2} = (1, 0, 0)$ and $\mathbf{E}_0 = (E_{0,x}(z, Z, T)e^{-i\omega t}, 0, 0)$. The non-homogeneous equation (3.5) at the x-component of the solution $\mathbf{E}_1$ at $e^{-i\omega t}$ takes the form:

$$\nabla^2 E_{1,x} + k^2 E_{1,x} = -2ik^2 \frac{\partial}{\partial T} E_{0,x} - 2k \frac{\partial^2}{\partial Z \partial z} E_{0,x} - \frac{2k^2 n_1(\mathbf{x})}{n_0} E_{0,x} + \frac{2}{n_0} \frac{\partial^2 n_1(\mathbf{x})}{\partial x^2} E_{0,x}.$$

By removing the resonant terms at $e^{\pm ikz}$, the coupled-mode equations for amplitudes $A_\pm(Z, T)$ take the form:

$$i\left(\frac{\partial A_+}{\partial T} + \frac{\partial A_+}{\partial Z}\right) + \alpha A_- = 0, \tag{3.8}$$

$$i\left(\frac{\partial A_-}{\partial T} - \frac{\partial A_-}{\partial Z}\right) + \alpha A_+ = 0, \tag{3.9}$$

where $\alpha = \alpha_{0,0,1} = \alpha_{0,0,-1}$. The coupled-mode equations (3.8)–(3.9) can be defined on the interval $0 \leq Z \leq L_z$ for $T \geq 0$, where the end points at $Z = 0$ and $Z = L_z$ are the left and right (x, y)-planes, which cut a slice of the photonic crystal. The linear system (3.8)–(3.9) is reviewed in [SS]. The nonlinear coupled-mode equations are derived in [BS, SSS] and analyzed recently in [GWH, PSBS, PS].

3.2 Coupled-mode equations for two-dimensional resonance

3.2.1 Coupled-mode equations for four counter-propagating waves

The lowest-order resonance for four counter-propagating waves (2.16) occurs for $p = q = 1$, when

$$\mathbf{k}_1 = \frac{\pi}{a}(1, 1, 0), \quad \mathbf{k}_2 = \frac{\pi}{a}(1, -1, 0), \tag{3.10}$$
$$\mathbf{k}_3 = \frac{\pi}{a}(-1, 1, 0), \quad \mathbf{k}_4 = \frac{\pi}{a}(-1, -1, 0).$$

Let $A_1 = A_+(X,Y,T)$ and $A_4 = A_-(X,Y,T)$ be the amplitudes of the counter-propagating waves along the main diagonal of the (x,y) plane, while $A_2 = B_+(X,Y,T)$ and $A_3 = B_-(X,Y,T)$ be the amplitudes of the counter-propagating waves along the anti-diagonal of the (x,y)-plane. The envelope amplitudes are not modulated in the Z-direction, since the coupled-mode equations for $A_\pm$ and $B_\pm$ are essentially two-dimensional. The polarization vectors are chosen in the z-direction, such that $\mathbf{e}_{\mathbf{k}_j} = (0,0,1)$, $1 \leq j \leq 4$, which corresponds to the TE mode of the photonic crystal, such that $\mathbf{E}_0 = (0,0,E_{0,z}(x,y,X,Y,T)e^{-i\omega t})$. The non-homogeneous equation (3.5) at the z-component of the solution $\mathbf{E}_1$ at $e^{-i\omega t}$ takes the form:

$$\begin{aligned} \nabla^2 E_{1,z} + k^2 E_{1,z} &= -2ik^2 \frac{\partial}{\partial T} E_{0,z} - 2k \frac{\partial^2}{\partial X \partial x} E_{0,z} - 2k \frac{\partial^2}{\partial Y \partial y} E_{0,z} \\ &- \frac{2k^2 n_1(\mathbf{x})}{n_0} E_{0,z} + \frac{2}{n_0} \frac{\partial^2 n_1(\mathbf{x})}{\partial z^2} E_{0,z}. \end{aligned} \tag{3.11}$$

By removing the resonant terms at $e^{\frac{i}{\sqrt{2}}(\pm kx \pm ky)}$, the coupled-mode equations for amplitudes $A_\pm(X,Y,T)$ and $B_\pm(X,Y,T)$ take the form:

$$i\left(\frac{\partial A_+}{\partial T} + \frac{\partial A_+}{\partial X} + \frac{\partial A_+}{\partial Y}\right) + \alpha A_- + \beta\left(B_+ + B_-\right) = 0, \tag{3.12}$$

$$i\left(\frac{\partial A_-}{\partial T} - \frac{\partial A_-}{\partial X} - \frac{\partial A_-}{\partial Y}\right) + \alpha A_+ + \beta\left(B_+ + B_-\right) = 0, \tag{3.13}$$

$$i\left(\frac{\partial B_+}{\partial T} + \frac{\partial B_+}{\partial X} - \frac{\partial B_+}{\partial Y}\right) + \beta\left(A_+ + A_-\right) + \alpha B_- = 0, \tag{3.14}$$

$$i\left(\frac{\partial B_-}{\partial T} - \frac{\partial B_-}{\partial X} + \frac{\partial B_-}{\partial Y}\right) + \beta\left(A_+ + A_-\right) + \alpha B_+ = 0, \tag{3.15}$$

where $\alpha = \alpha_{1,1,0} = \alpha_{-1,-1,0} = \alpha_{1,-1,0} = \alpha_{-1,1,0}$ and $\beta = \alpha_{0,1,0} = \alpha_{1,0,0} = \alpha_{0,-1,0} = \alpha_{-1,0,0}$. The coupled-mode equations (3.12)–(3.15) can be defined in the domain $(X,Y) \in \mathcal{D}$ and $T \geq 0$, where $\mathcal{D}$ is a domain on the (x,y)-plane of the photonic crystal. The system has not been previously studied in literature, to the best of our knowledge.

3.2.2 Second and higher order resonance for four counter-propagating waves in two-dimensional cubic crystal

The coupled-mode equations (3.12)–(3.15) for four counter-propagating waves derived in the first order Bragg resonance. We show here that the higher order Bragg resonances it 2D crystal can give the same coupled-mode system of four counter-propagating waves.

Consider second order Bragg resonance on the (x, y) plane with $\mathbf{k}_{in} = \frac{2\pi}{a}(1, 0)$, as can be seen in Figure 2.4 there are three lattice vectors $\mathbf{G}$ that are in resonance with $\mathbf{k}_{in} = \frac{2\pi}{a}(1, 0)$

$$\begin{aligned} \mathbf{G}_1 &= \frac{2\pi}{a}(2, 0) \\ \mathbf{G}_2 &= \frac{2\pi}{a}(1, -1) \\ \mathbf{G}_3 &= \frac{2\pi}{a}(1, 1) \end{aligned}$$

Hence there are four resonant counter-propagating waves, that are given by wave-vectors

$$\begin{aligned} \mathbf{k} &= \frac{2\pi}{a}(1, 0) \\ \mathbf{k} - \mathbf{G}_1 &= \frac{2\pi}{a}(-1, 0) \\ \mathbf{k} - \mathbf{G}_2 &= \frac{2\pi}{a}(0, 1) \\ \mathbf{k} - \mathbf{G}_3 &= \frac{2\pi}{a}(0, -1) \end{aligned}$$

It can be seen from the Figure 3.1 that another basis cell can be use for the same crystal. We introduce new dual lattice $\mathbf{k}'_1, \mathbf{k}'_2$, which is rotated about the basis $\mathbf{k}_1, \mathbf{k}_2$.

$$\mathbf{k}'_1 = \mathbf{k}_1 + \mathbf{k}_2$$

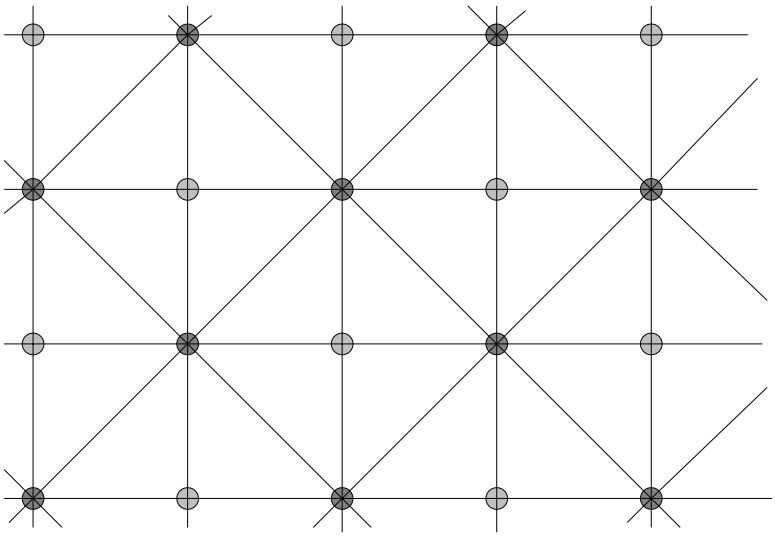

Figure 3.1: The same two-dimensional cubic crystal can be obtained by translation of two basis cells. The basis cell we the smallest volume is called primitive.

$$\mathbf{k}_2' = \mathbf{k}_2 - \mathbf{k}_1$$

The triple Fourier series for n(x) is now

$$n(x) = \sum_{\mathbf{G}'} \alpha'_{\mathbf{G}'} e^{i\mathbf{G}'\mathbf{x}}$$

Where $\mathbf{G}'$ lies in the new dual lattice $\mathbf{G}' = n\mathbf{k}_1' + m\mathbf{k}_2'$.

Now the derivation of coupled-mode equations for four counter-propagating waves in the first Bragg resonance can be repeated to obtain the coupled-mode equations for four counter-propagating waves in the second Bragg resonance in 2D crystals with obvious change $\alpha \to \alpha'$.

Let $A_1 = A_+(X,Y,T)$ and $A_2 = A_-(X,Y,T)$ be the amplitudes of the counter-propagating waves in x direction, while $A_3 = B_+(X,Y,T)$ and $A_4 = B_-(X,Y,T)$ be the amplitudes of the counter-propagating waves in y direction. The envelope amplitudes are not modulated in the Z-direction, since the coupled-mode equations for $A_\pm$ and $B_\pm$ are essentially two-dimensional. We obtain the coupled-mode equations

for amplitudes $A_{\pm}(X,Y,T)$ and $B_{\pm}(X,Y,T)$:

$$i\left(\frac{\partial A_+}{\partial T}+\frac{\partial A_+}{\partial X}\right)+\alpha' A_- +\beta'\left(B_+ + B_-\right) = 0, \tag{3.16}$$

$$i\left(\frac{\partial A_-}{\partial T}-\frac{\partial A_-}{\partial X}\right)+\alpha' A_+ +\beta'\left(B_+ + B_-\right) = 0, \tag{3.17}$$

$$i\left(\frac{\partial B_+}{\partial T}+\frac{\partial B_+}{\partial Y}\right)+\beta'\left(A_+ + A_-\right)+\alpha' B_- = 0, \tag{3.18}$$

$$i\left(\frac{\partial B_-}{\partial T}-\frac{\partial B_-}{\partial Y}\right)+\beta'\left(A_+ + A_-\right)+\alpha' B_+ = 0, \tag{3.19}$$

where $\alpha' = \alpha'_{1,1,0} = \alpha'_{-1,-1,0} = \alpha'_{1,-1,0} = \alpha'_{-1,1,0}$ and $\beta' = \alpha'_{0,1,0} = \alpha'_{1,0,0} = \alpha'_{0,-1,0} = \alpha'_{-1,0,0}$. The explicit formula for α' in terms of α is

$$\alpha'_{n,m} = \alpha_{n-m,n+m}$$

We conclude the treatment of two-dimensional photonic crystals with a simple algebraic theorem which is almost obvious from geometric construction on Figure 2.4.

Theorem 3.1 *All orthogonal counter propagating resonant waves in 2D cubic crystal occur for* $\mathbf{k}_{in} = \frac{2\pi}{a}(\frac{p+s}{2}, \frac{p-s}{2})$*, where* p, s *are integers.*

Proof. It is clear that the only parallel resonant waves allowed in photonic crystal are counter propagating waves. In order to find two orthogonal pairs of counter-propagating waves we have to solve the system

$$\begin{aligned} |k| &= |k+G| \\ k &\perp (k+G) \end{aligned}$$

Denote $k = (k_1, k_2)$, $G = (n, m)$, the system transforms to

$$k_1^2 + k_2^2 = (n+k_1)^2 + (m+k_2)^2$$

$$k_1(k_1+n) + k_2(k_2+m) = 0$$

Expressing m in terms of n from the second equation we get

$$(n + k_1)^2 = k_2^2$$
$$m = -\frac{k_1(k_1 + n) + k_2^2}{k_2}$$

This gives us two sets of solutions

$$n_1 = k_2 - k_1, \qquad m_1 = -k_2 - k_1$$
$$n_2 = -k_2 - k_1, \qquad m_2 = -k_2 + k_1$$

It is easy to see that this two sets describe two orthogonal vectors G_1 and G_2. For this vectors to lie on the reciprocal lattice we require

$$k_1 = \frac{p + s}{2}$$
$$k_2 = \frac{p - s}{2},$$

where p and s are integers. The theorem is now proven. ■

The theorem gives us necessary and sufficient condition for existence of four orthogonal counter-propagating resonant waves.

It is not clear for what k_{in}, in general, there are *only* four non-orthogonal counter propagating waves in cubic crystal. The obvious necessary condition for that is $k_{in} = \frac{2\pi}{a}(p, s)$ where $p, s \in \mathbb{Z}^2$.

3.3 Coupled-mode equations for two oblique waves

Two oblique resonant waves on the (x, y)-plane are defined by the resonant wave vectors (2.17) under the constraint (2.18). Assuming that $\mathbf{e}_1 = \mathbf{e}_2 = (0, 0, 1)$, the Maxwell equations can be reduced to the same form (3.11), where the resonant terms

are eliminated at the wave vectors $\mathbf{k}_1 = \mathbf{k}_{\rm in}$ and $\mathbf{k}_2 = \mathbf{k}_{\rm out}^{(n,m,0)}$. The coupled-mode equations for amplitudes $A_{1,2}(X,Y,T)$ take the form:

$$i\left(\frac{\partial A_1}{\partial T} + \frac{p}{\sqrt{p^2+q^2}}\frac{\partial A_1}{\partial X} + \frac{q}{\sqrt{p^2+q^2}}\frac{\partial A_1}{\partial Y}\right) + \alpha A_2 = 0, \tag{3.20}$$

$$i\left(\frac{\partial A_2}{\partial T} + \frac{p+2n}{\sqrt{p^2+q^2}}\frac{\partial A_2}{\partial X} + \frac{q+2m}{\sqrt{p^2+q^2}}\frac{\partial A_2}{\partial Y}\right) + \alpha A_1 = 0. \tag{3.21}$$

where $\alpha = \alpha_{n,m,0} = \alpha_{-n,-m,0}$. Coupled-mode equations (3.20)–(3.21) for two oblique waves can not be reduced to the one-dimensional system (3.8)–(3.9), since the characteristics in the system (3.20)–(3.21) are no longer parallel.

The coupled-mode equations for three oblique resonant waves (2.19) can be derived similarly, subject to the resonance condition (2.20). Three characteristics along the wave vectors $\mathbf{k}_1 = \mathbf{k}_{\rm in}$, $\mathbf{k}_2 = \mathbf{k}_{\rm out}^{(n_1,m_1,0)}$, and $\mathbf{k}_3 = \mathbf{k}_{\rm out}^{(n_2,m_2,0)}$ belong to the same (X,Y)-plane. The stationary transmission problem for the three oblique waves is hence a boundary-value problem on the (X,Y)-plane with three (linearly dependent) characteristic coordinates. Oblique interaction of three oblique resonant Bloch waves in a hexagonal crystal was considered numerically in [SGS].

3.4 Coupled-mode equations for six counter-propagating waves in 3D photonic crystal

The lowest-order resonance for six counter-propagating waves occurs for $p = 2, q = r = 0$, when

$$\begin{aligned} \mathbf{k}_1 &= \frac{2\pi}{a}(1,0,0) \\ \mathbf{k}_2 &= \frac{2\pi}{a}(-1,0,0) \\ \mathbf{k}_3 &= \frac{2\pi}{a}(0,1,0) \end{aligned}$$

$$\begin{aligned}
\mathbf{k}_4 &= \frac{2\pi}{a}(0,-1,0)\\
\mathbf{k}_5 &= \frac{2\pi}{a}(0,0,1)\\
\mathbf{k}_6 &= \frac{2\pi}{a}(0,0,-1)
\end{aligned}$$

Let $A_1 = A_+(X,Y,Z,T)$ and $A_2 = A_-(X,Y,Z,T)$ be the amplitudes of the counter-propagating waves in x direction, while $A_3 = B_+(X,Y,Z,T)$ and $A_4 = B_-(X,Y,Z,T)$ be the amplitudes of the counter-propagating waves in y direction, $A_5 = C_+(X,Y,Z,T)$ and $A_6 = C_-(X,Y,Z,T)$ be the amplitudes of the counter-propagating waves in z direction. This resonance is fully three-dimensional.

Substituting into the non-homogeneous equation (3.5) and removing resonant terms for solution $\mathbf{E}_1$ at $e^{i\pm kx},\ e^{i\pm ky},\ e^{i\pm kz}$ the coupled-mode equations for the amplitudes $A_\pm(X,Y,ZT)$, $B_\pm(X,Y,Z,T)$ and $C_\pm(X,Y,Z,T)$ take the form:

$$\begin{aligned}
&i\ \left(\frac{\partial A_+}{\partial T}+\frac{\partial A_+}{\partial X}\right)+\alpha_{2,0,0}A_-+\alpha_{1,-1,0}B_++\alpha_{1,1,0}B_-+\alpha_{1,0,-1}C_++\alpha_{1,0,1}C_-=0,\\
&i\ \left(\frac{\partial A_-}{\partial T}-\frac{\partial A_-}{\partial X}\right)+\alpha_{-2,0,0}A_++\alpha_{-1,-1,0}B_++\alpha_{-1,1,0}B_-+\alpha_{-1,0,-1}C_++\alpha_{-1,0,1}C_-=0,\\
&i\ \left(\frac{\partial B_+}{\partial T}+\frac{\partial B_+}{\partial Y}\right)+\alpha_{-1,1,0}A_++\alpha_{1,1,0}A_-+\alpha_{0,2,0}B_-+\alpha_{0,1,-1}C_++\alpha_{0,1,1}C_-=0,\\
&i\ \left(\frac{\partial B_-}{\partial T}-\frac{\partial B_-}{\partial Y}\right)+\alpha_{-1,-1,0}A_++\alpha_{1,-1,0}A_-+\alpha_{0,-2,0}B_++\alpha_{0,-1,-1}C_++\alpha_{0,-1,1}C_-=0,\\
&i\ \left(\frac{\partial C_+}{\partial T}+\frac{\partial C_+}{\partial Z}\right)+\alpha_{-1,0,1}A_++\alpha_{1,0,1}A_-+\alpha_{0,-1,1}B_++\alpha_{0,1,1}B_-+\alpha_{0,0,2}C_-=0,\\
&i\ \left(\frac{\partial C_-}{\partial T}-\frac{\partial C_-}{\partial Z}\right)+\alpha_{-1,0,-1}A_++\alpha_{1,0,-1}A_-+\alpha_{0,-1,-1}B_++\alpha_{0,1,-1}B_-+\alpha_{0,0,-2}C_+=0
\end{aligned}$$

Due to the crystal symmetry we denote $\alpha = \alpha_{2,0,0}$ and $\beta = \alpha_{1,1,0}$ and rewrite the system as

$$i\ \left(\frac{\partial A_+}{\partial T}+\frac{\partial A_+}{\partial X}\right)+\alpha A_-+\beta(B_++B_-+C_++C_-)=0, \tag{3.22}$$

$$i\left(\frac{\partial A_-}{\partial T}-\frac{\partial A_-}{\partial X}\right)+\alpha A_+ +\beta(B_+ + B_- + C_+ + C_-)=0, \tag{3.23}$$

$$i\left(\frac{\partial B_+}{\partial T}+\frac{\partial B_+}{\partial Y}\right)+\alpha B_- +\beta(A_+ + A_- + C_+ + C_-)=0, \tag{3.24}$$

$$i\left(\frac{\partial B_-}{\partial T}-\frac{\partial B_-}{\partial Y}\right)+\alpha B_+ +\beta(A_+ + A_- + C_+ + C_-)=0, \tag{3.25}$$

$$i\left(\frac{\partial C_+}{\partial T}+\frac{\partial C_+}{\partial Z}\right)+\alpha C_- +\beta(A_+ + A_- + B_+ + B_-)=0, \tag{3.26}$$

$$i\left(\frac{\partial C_-}{\partial T}-\frac{\partial C_-}{\partial Z}\right)+\alpha C_+ +\beta(A_+ + A_- + B_+ + B_-)=0. \tag{3.27}$$

The coupled-mode equations (3.22)–(3.27) can be defined in the domain $(X, Y, Z) \in \mathcal{D}$ and $T \geq 0$, where $\mathcal{D}$ is a domain on the (x, y, z)-space of the photonic crystal. The system has not been previously studied in literature, to the best of our knowledge. The reduction of the system to the (x, y) plane gives the system (3.16)–(3.19).

3.5 Nonlinear coupled-mode equations with cubic nonlinearities

Modeling of nonlinear photonic band-gap crystals with cubic (Kerr) nonlinearities is based on the Maxwell equations, where the polarization vector depends nonlinearly from the electric field vector $\mathbf{E}$ [K2]. When the nonlinearity terms are small, nonlocal (dispersive) terms in the polarization vector can be neglected and the low-contrast weakly-nonlinear photonic crystals can be modelled with the Maxwell equations (2.1), where the refractive index $n = n(\mathbf{x}, |\mathbf{E}|^2)$ is decomposed into the linear and nonlinear parts [SS]:

$$n(\mathbf{x}, |\mathbf{E}|^2) = n_0 + \epsilon n_1(\mathbf{x}) + \epsilon n_2(\mathbf{x})|\mathbf{E}|^2, \tag{3.28}$$

where n_0 is constant and ϵ is small parameter. When the photonic crystal has cubic-lattice structure, the periodic functions $n_1(\mathbf{x})$ and $n_2(\mathbf{x})$ are expanded into the triple

Fourier series (3.4) and

$$n_2(\mathbf{x}) = n_0 \sum_{(n,m,l)\in\mathbb{Z}^3} \beta_{n,m,l} e^{ik_0(nx+my+lz)}, \tag{3.29}$$

where the factor n_0 is included for convenience. The Fourier coefficients $\beta_{n,m,l}$ satisfy the same symmetries as α under condition that $n(\mathbf{x})$ is invariant with respect to crystal symmetries. It follows that all coefficients $\beta_{n,m,l}$ for $(n,m,l) \in \mathbb{Z}^3$ are real-valued.

Derivation of the nonlinear coupled-mode equations is based on rigorous methods of Lyapunov-Schmidt reductions [SU]. Equivalently, the formal derivation can be recovered with the perturbation series expansions [Sh], which follows to the formalism (3.2) and (3.3). The first-order correction term $\mathbf{E}_1(\mathbf{x},t)$ solves the non-homogeneous problem (3.5) with additional nonlinear terms:

$$\begin{aligned} \nabla^2\mathbf{E}_1 - \frac{n_0^2}{c^2}\frac{\partial^2\mathbf{E}_1}{\partial t^2} &= 2\frac{n_0^2\omega}{c^2}\frac{\partial^2\mathbf{E}_0}{\partial T\partial t} - 2k\left(\nabla\cdot\nabla_X\right)\mathbf{E}_0 + \frac{2n_0n_1(\mathbf{x})}{c^2}\frac{\partial^2\mathbf{E}_0}{\partial t^2} + \frac{2}{n_0}\nabla\left(\nabla n_1\cdot\mathbf{E}_0\right) \\ &+ \frac{2n_0n_2(\mathbf{x})}{c^2}|\mathbf{E}_0|^2\frac{\partial^2\mathbf{E}_0}{\partial t^2} + \frac{2}{n_0}\nabla\left(\nabla n_2|\mathbf{E}_0|^2\cdot\mathbf{E}_0\right). \end{aligned} \tag{3.30}$$

The cubic nonlinear terms generates N^3 terms from the leading-order solution (3.3), which all give resonant terms by means of the triple series (3.29). By removing the resonant terms, the nonlinear coupled-mode equations for $A_j(\mathbf{X},T)$, $j = 1,...,N$ are derived in the general form:

$$\begin{aligned} 2ik^2\left(\frac{\partial A_j}{\partial T} + \left(\frac{\mathbf{k}_j}{k}\cdot\nabla_X\right)A_j\right) + \sum_{k\neq j} a_{j,k}A_k \\ + \sum_{1\leq k_1,k_2,k_3\leq N} b_{j,k_1,k_2,k_3}A_{k_1}A_{k_2}\bar{A}_{k_3} = 0, \end{aligned} \tag{3.31}$$

where the elements $\{b_{j,k_1,k_2,k_3}\}_{1\leq j,k_1,k_2,k_3\leq N}$ are related to the Fourier coefficients $\{\beta_{n,m,l}\}_{(n,m,l)\in\mathbb{Z}^3}$ at the resonant terms $(n,m,l) \in \mathcal{S}$. The explicit forms of the nonlinear coupled-mode equations are given below for two and four counter-propagating and two oblique resonant Bloch waves.

The nonlinear coupled mode equations for two counter-propagating waves (3.7) generalize the linear equations (3.8)–(3.9) as follows:

$$\begin{aligned}
i\left(\frac{\partial A_+}{\partial T}+\frac{\partial A_+}{\partial Z}\right) &+ \alpha A_- + \beta_{0,0,0}\left(|A_+|^2+2|A_-|^2\right)A_+ \\
&+ \beta_{0,0,1}\left(2|A_+|^2+|A_-|^2\right)A_- + \beta_{0,0,-1}A_+^2\bar{A}_- + \beta_{0,0,2}\bar{A}_+A_-^2 = 0, \\
i\left(\frac{\partial A_-}{\partial T}-\frac{\partial A_-}{\partial Z}\right) &+ \alpha A_+ + \beta_{0,0,0}\left(2|A_+|^2+|A_-|^2\right)A_- \\
&+ \beta_{0,0,-1}\left(|A_+|^2+2|A_-|^2\right)A_+ + \beta_{0,0,1}\bar{A}_+A_-^2 + \beta_{0,0,-2}A_+^2\bar{A}_- = 0.
\end{aligned}$$

The system (3.32)–(3.32) is reviewed in [GWH, SS] for $\beta_{0,0,1} = \beta_{0,0,2} = 0$ and analyzed in [PSBS, PS] for $\beta_{0,0,1} \neq 0$ and $\beta_{0,0,2} = 0$. When $\beta_{0,0,1}, \beta_{0,0,2} \neq 0$, the system (3.8)–(3.9) is the most general coupled-mode system for Bragg resonance of two counter-propagating waves [BS, SSS].

The nonlinear coupled-mode equations for four counter-propagating waves (3.10) generalize the linear equations (3.12)–(3.15) as follows:

$$\begin{aligned}
i\left(\frac{\partial A_+}{\partial T}+\frac{\partial A_+}{\partial X}+\frac{\partial A_+}{\partial Y}\right)+\alpha A_-+\beta\left(B_++B_-\right)+F_+(A_+,A_-,B_+,B_-) &= 0, \\
i\left(\frac{\partial A_-}{\partial T}-\frac{\partial A_-}{\partial X}-\frac{\partial A_-}{\partial Y}\right)+\alpha A_++\beta\left(B_++B_-\right)+F_-(A_+,A_-,B_+,B_-) &= 0, \\
i\left(\frac{\partial B_+}{\partial T}+\frac{\partial B_+}{\partial X}-\frac{\partial B_+}{\partial Y}\right)+\beta\left(A_++A_-\right)+\alpha B_-+G_+(A_+,A_-,B_+,B_-) &= 0, \\
i\left(\frac{\partial B_-}{\partial T}-\frac{\partial B_-}{\partial X}+\frac{\partial B_-}{\partial Y}\right)+\beta\left(A_++A_-\right)+\alpha B_++G_-(A_+,A_-,B_+,B_-) &= 0,
\end{aligned}$$

where the cubic nonlinear functions are given by

$$\begin{aligned}
F_+ &= \beta_{0,0,0}\left((|A_+|^2+2|A_-|^2+2|B_+|^2+2|B_-|^2)A_+ + 2\bar{A}_-B_+B_-\right) + \beta_{0,-1,0}\left(A_+^2\bar{B}_+ + 2A_+\bar{A}_-B_-\right) \\
&+ \beta_{1,1,0}\left((2|A_+|^2+|A_-|^2+2|B_+|^2+2|B_-|^2)A_- + 2\bar{A}_+B_+B_-\right) + \beta_{-1,0,0}\left(A_+^2\bar{B}_- + 2A_+\bar{A}_-B_+\right) \\
&+ \beta_{0,1,0}\left((2|A_+|^2+2|A_-|^2+|B_+|^2+2|B_-|^2)B_+ + 2A_+A_-\bar{B}_-\right) + \beta_{-1,1,0}\left(2A_+B_+\bar{B}_- + \bar{A}_-B_+^2\right) \\
&+ \beta_{1,0,0}\left((2|A_+|^2+2|A_-|^2+2|B_+|^2+|B_-|^2)B_- + 2A_+A_-\bar{B}_+\right) + \beta_{1,-1,0}\left(2A_+\bar{B}_+B_- + \bar{A}_-B_-^2\right) \\
&+ \beta_{2,0,0}\left(\bar{A}_+B_-^2 + 2A_-\bar{B}_+B_-\right) + \beta_{2,1,0}\left(2\bar{A}_+A_-B_- + A_-^2\bar{B}_+\right) + \beta_{1,2,0}\left(A_-^2\bar{B}_- + 2\bar{A}_+A_-B_+\right) \\
&+ \beta_{0,2,0}\left(\bar{A}_+B_+^2 + 2A_-B_+\bar{B}_-\right) + \beta_{-1,-1,0}A_+^2\bar{A}_- + \beta_{2,2,0}\bar{A}_+A_-^2 + \beta_{2,-1,0}\bar{B}_+B_-^2 + \beta_{-1,2,0}B_+^2\bar{B}_-,
\end{aligned}$$

$$F_- = \beta_{-1,-1,0}\left((|A_+|^2+2|A_-|^2+2|B_+|^2+2|B_-|^2)A_+ + 2\bar{A}_-B_+B_-\right) + \beta_{-1,-2,0}\left(A_+^2\bar{B}_+ + 2A_+\bar{A}_-B_-\right)$$

$$
\begin{aligned}
&+ \beta_{0,0,0}\left((2|A_+|^2+|A_-|^2+2|B_+|^2+2|B_-|^2)A_- + 2\bar{A}_+B_+B_-\right) + \beta_{-2,-1,0}\left(A_+^2\bar{B}_- + 2A_+\bar{A}_-B_+\right)\\
&+ \beta_{-1,0,0}\left((2|A_+|^2+2|A_-|^2+|B_+|^2+2|B_-|^2)B_+ + 2A_+A_-\bar{B}_-\right) + \beta_{-2,0,0}\left(2A_+B_+\bar{B}_- + \bar{A}_-B_+^2\right)\\
&+ \beta_{0,-1,0}\left((2|A_+|^2+2|A_-|^2+2|B_+|^2+|B_-|^2)B_- + 2A_+A_-\bar{B}_+\right) + \beta_{0,-2,0}\left(2A_+\bar{B}_+B_- + \bar{A}_-B_-^2\right)\\
&+ \beta_{1,-1,0}\left(\bar{A}_+B_-^2 + 2A_-\bar{B}_+B_-\right) + \beta_{1,0,0}\left(2\bar{A}_+A_-B_- + A_-^2\bar{B}_+\right) + \beta_{0,1,0}\left(A_-^2\bar{B}_- + 2\bar{A}_+A_-B_+\right)\\
&+ \beta_{-1,1,0}\left(\bar{A}_+B_+^2 + 2A_-B_+\bar{B}_-\right) + \beta_{-2,-2,0}A_+^2\bar{A}_- + \beta_{1,1,0}\bar{A}_+A_-^2 + \beta_{1,-2,0}\bar{B}_+B_-^2 + \beta_{-2,1,0}B_+^2\bar{B}_-,
\end{aligned}
$$

$$
\begin{aligned}
G_+ &= \beta_{0,-1,0}\left((|A_+|^2+2|A_-|^2+2|B_+|^2+2|B_-|^2)A_+ + 2\bar{A}_-B_+B_-\right) + \beta_{0,-2,0}\left(A_+^2\bar{B}_+ + 2A_+\bar{A}_-B_-\right)\\
&+ \beta_{1,0,0}\left((2|A_+|^2+|A_-|^2+2|B_+|^2+2|B_-|^2)A_- + 2\bar{A}_+B_+B_-\right) + \beta_{-1,-1,0}\left(A_+^2\bar{B}_- + 2A_+\bar{A}_-B_+\right)\\
&+ \beta_{0,0,0}\left((2|A_+|^2+2|A_-|^2+|B_+|^2+2|B_-|^2)B_+ + 2A_+A_-\bar{B}_-\right) + \beta_{-1,0,0}\left(2A_+B_+\bar{B}_- + \bar{A}_-B_+^2\right)\\
&+ \beta_{1,-1,0}\left((2|A_+|^2+2|A_-|^2+2|B_+|^2+|B_-|^2)B_- + 2A_+A_-\bar{B}_+\right) + \beta_{1,-2,0}\left(2A_+\bar{B}_+B_- + \bar{A}_-B_-^2\right)\\
&+ \beta_{2,-1,0}\left(\bar{A}_+B_-^2 + 2A_-\bar{B}_+B_-\right) + \beta_{2,0,0}\left(2\bar{A}_+A_-B_- + A_-^2\bar{B}_+\right) + \beta_{1,1,0}\left(A_-^2\bar{B}_- + 2\bar{A}_+A_-B_+\right)\\
&+ \beta_{0,1,0}\left(\bar{A}_+B_+^2 + 2A_-B_+\bar{B}_-\right) + \beta_{-1,-2,0}A_+^2\bar{A}_- + \beta_{2,1,0}\bar{A}_+A_-^2 + \beta_{2,-2,0}\bar{B}_+B_-^2 + \beta_{-1,1,0}B_+^2\bar{B}_-,
\end{aligned}
$$

$$
\begin{aligned}
G_- &= \beta_{-1,0,0}\left((|A_+|^2+2|A_-|^2+2|B_+|^2+2|B_-|^2)A_+ + 2\bar{A}_-B_+B_-\right) + \beta_{-1,-1,0}\left(A_+^2\bar{B}_+ + 2A_+\bar{A}_-B_-\right)\\
&+ \beta_{0,1,0}\left((2|A_+|^2+|A_-|^2+2|B_+|^2+2|B_-|^2)A_- + 2\bar{A}_+B_+B_-\right) + \beta_{-2,0,0}\left(A_+^2\bar{B}_- + 2A_+\bar{A}_-B_+\right)\\
&+ \beta_{-1,1,0}\left((2|A_+|^2+2|A_-|^2+|B_+|^2+2|B_-|^2)B_+ + 2A_+A_-\bar{B}_-\right) + \beta_{-2,1,0}\left(2A_+B_+\bar{B}_- + \bar{A}_-B_+^2\right)\\
&+ \beta_{0,0,0}\left((2|A_+|^2+2|A_-|^2+2|B_+|^2+|B_-|^2)B_- + 2A_+A_-\bar{B}_+\right) + \beta_{0,-1,0}\left(2A_+\bar{B}_+B_- + \bar{A}_-B_-^2\right)\\
&+ \beta_{1,0,0}\left(\bar{A}_+B_-^2 + 2A_-\bar{B}_+B_-\right) + \beta_{1,1,0}\left(2\bar{A}_+A_-B_- + A_-^2\bar{B}_+\right) + \beta_{0,2,0}\left(A_-^2\bar{B}_- + 2\bar{A}_+A_-B_+\right)\\
&+ \beta_{-1,2,0}\left(\bar{A}_+B_+^2 + 2A_-B_+\bar{B}_-\right) + \beta_{-2,-1,0}A_+^2\bar{A}_- + \beta_{1,2,0}\bar{A}_+A_-^2 + \beta_{1,-1,0}\bar{B}_+B_-^2 + \beta_{-2,2,0}B_+^2\bar{B}_-.
\end{aligned}
$$

The nonlinear coupled-mode equations for two oblique waves (2.17) generalize the linear equations (3.20)–(3.21) as follows:

$$
\begin{aligned}
&i\left(\frac{\partial A_1}{\partial T} + \frac{p}{\sqrt{p^2+q^2}}\frac{\partial A_1}{\partial X} + \frac{q}{\sqrt{p^2+q^2}}\frac{\partial A_1}{\partial Y}\right) + \alpha A_2 + \beta_{0,0,0}\left(|A_1|^2+2|A_2|^2\right)A_1\\
&\qquad + \beta_{-n,-m,0}\left(2|A_1|^2+|A_2|^2\right)A_2 + \beta_{n,m,0}A_1^2\bar{A}_2 + \beta_{-2n,-2m,0}\bar{A}_1A_2^2 = 0,
\end{aligned}
\tag{3.32}
$$

$$
\begin{aligned}
&i\left(\frac{\partial A_2}{\partial T} + \frac{p+2n}{\sqrt{p^2+q^2}}\frac{\partial A_2}{\partial X} + \frac{q+2m}{\sqrt{p^2+q^2}}\frac{\partial A_2}{\partial Y}\right) + \alpha A_1 + \beta_{0,0,0}\left(2|A_1|^2+|A_2|^2\right)A_1\\
&\qquad + \beta_{n,m,0}\left(|A_1|^2+2|A_2|^2\right)A_1 + \beta_{-n,-m,0}\bar{A}_1A_2^2 + \beta_{2n,2m,0}A_1^2\bar{A}_2 = 0.
\end{aligned}
\tag{3.33}
$$

The system (3.32)–(3.33) and its generalization to three oblique resonant waves are reviewed in [SGS, Sh].

Chapter 4

Analysis of stationary transmission

The stationary transmission problem follows from the separation of variables in the coupled-mode equations (3.6):

$$A_j(\mathbf{X}, T) = a_j(\mathbf{X})e^{-i\Omega T}, \qquad j = 1, ..., N, \tag{4.1}$$

where Ω is the detuning frequency.

First, we prove the existence and uniqueness theorem for the solution of coupled-mode equations for four counter propagating waves. We start with a linear case, generalize the proof to include Lipschitz nonlinearities, and conclude with the proof of existence and uniqueness of solution in the case of Kerr nonlinearity under the condition of small domain. Finally the theorem is generalized for N-wave resonance.

4.1 Existence and uniqueness of solutions for four counter-propagating waves

We start with the example of stationary transmission of four counter-propagating waves. The system (3.16)–(3.19) after separation of variables (4.1) is simplified as follows:

$$i\frac{\partial a_+}{\partial x} + \Omega a_+ + \alpha a_- + \beta\,(b_+ + b_-) = 0, \tag{4.2}$$

$$-i\frac{\partial a_-}{\partial x} + \alpha a_+ + \Omega a_- + \beta\,(b_+ + b_-) = 0, \tag{4.3}$$

$$i\frac{\partial b_+}{\partial y} + \beta\,(a_+ + a_-) + \Omega b_+ + \alpha b_- = 0, \tag{4.4}$$

$$-i\frac{\partial b_-}{\partial y} + \beta\,(a_+ + a_-) + \alpha b_+ + \Omega b_- = 0. \tag{4.5}$$

Let us define the problem (4.2)–(4.5) on the rectangle,

$$\mathcal{D} = \{(x, y) :\ 0 \le x \le L,\ 0 \le y \le H\},$$

subject to the boundary conditions:

$$a_+(0, y) = a_+(y), \qquad a_-(L, y) = a_-(y), \qquad b_+(x, 0) = b_+(x), \qquad b_-(x, H) = b_-(x), \tag{4.6}$$

where $a_+(y), a_-(y), b_+(x), b_-(x)$ are given amplitudes of the incident waves at the left, right, bottom and top boundaries of the crystal. The geometry of the problem is shown on the Figure 4.1.

To prove existence and uniqueness of the solution of the system (4.2)–(4.5) with boundary condition (4.6) we use the following facts [KF]

- Let A be a continuous map of complete metric space R into itself such that some power of it $B = A^n$ is a contraction; then the equation $Au = u$ has a unique solution.

- The space R of continuous vector functions $\mathbf{v}(x, y)$ on the compact domain with the norm $\rho(\mathbf{v}_1, \mathbf{v}_2) = \max_{x,y,i} |v_1^i(x, y) - v_2^i(x, y)|$ is complete.

Theorem 4.1 *There exist a unique solution of the system (4.2)–(4.5) in the domain $\mathcal{D}$ that satisfy boundary condition (4.6).*

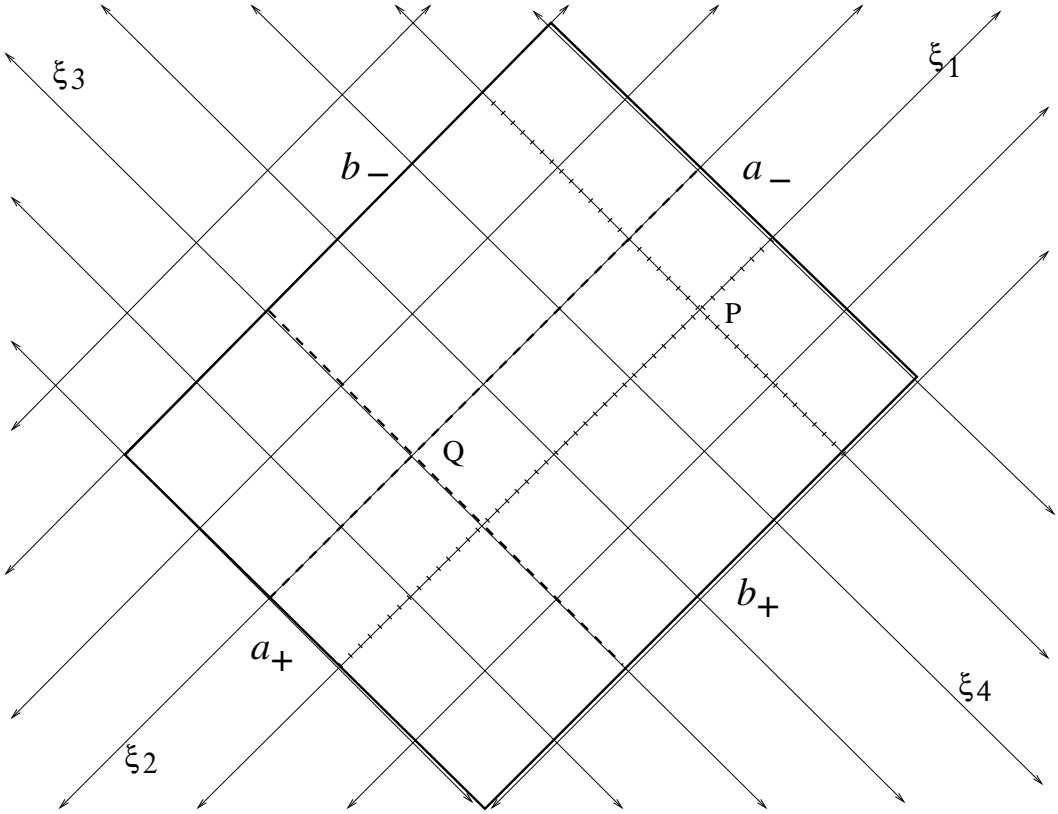

Figure 4.1: Four counter-propagating waves on the plane. The direction of the characteristics is shown with the arrowed lines. The characteristics that are going through points P and Q are shown with dashed lines. The wave a_+ propagates along ξ_1, a_- along ξ_2, b_+ along ξ_3 and b_- along ξ_4. The boundary data for this particular geometry of domain $\mathcal{D}$ is shown. For this case we will find the explicit solution of linear problem by separation of variables in the next chapter.

Proof. The system (4.2)–(4.5) with boundary condition (4.6) is equivalent to

$$
\begin{aligned}
a_+(x,y) &= a_+(0,y) + \int_0^x (\Omega a_+ + \alpha a_- + \beta(b_+ + b_-))\,dx \\
a_-(x,y) &= a_-(L,y) + \int_L^x (\alpha a_+ + \Omega a_- + \beta(b_+ + b_-))\,dx \\
b_+(x,y) &= a_+(x,0) + \int_0^y (\beta(a_+ + a_-) + \Omega b_+ + \alpha b_-)\,dy \\
b_-(x,y) &= b_-(x,H) + \int_H^y (\beta(a_+ + a_-) + \alpha b_+ + \Omega b_-)\,dy
\end{aligned}
$$

Hence, each component of the vector field

$$\begin{pmatrix} v^1 \\ v^2 \\ v^3 \\ v^4 \end{pmatrix} = \begin{pmatrix} a_+(x,y) \\ a_-(x,y) \\ b_+(x,y) \\ b_-(x,y) \end{pmatrix}$$

is expressed by a corresponding integral over the characteristic. To construct the solution we view the the integral system as a fixed point of the iteration problem.

$$\begin{aligned} v^1_{n+1}(x,y) &= a_+(0,y) + \int_0^x (\Omega v^1_n + \alpha v^2_n + \beta(v^3_n + v^4_n))\, dx \\ v^2_{n+1}(x,y) &= a_-(L,y) + \int_L^x (\alpha v^1_n + \Omega v^2_n + \beta(v^3_n + v^4_n))\, dx \\ v^3_{n+1}(x,y) &= a_+(x,0) + \int_0^y (\beta(v^1_n + v^2_n) + \Omega v^3_n + \alpha v^4_n)\, dy \\ v^4_{n+1}(x,y) &= b_-(x,H) + \int_H^y (\beta(v^1_n + v^2_n) + \alpha v^3_n + \Omega v^4_n)\, dy \end{aligned}$$

or symbolically

$$\mathbf{v}_{n+1} = A\mathbf{v}_n \qquad \text{where } A \text{ is the integral operator}$$

To apply the contraction mapping principle we want to show that some power of the map A is a contraction map. Let $\mathbf{v}_1$ and $\mathbf{v}_2$ be two continuous vector fields on $\mathcal{D} = \{(x,y) :\ 0 \le x \le L,\ 0 \le y \le H\}$, define metrics

$$\rho(\mathbf{v}_1, \mathbf{v}_2) = \max_{x,y,i} |v^i_1(x,y) - v^i_2(x,y)|$$

Hence, we use the *maximum norm* $\|\mathbf{v}\|$ of a continuous vector field $\mathbf{v}$, that is, the largest value of $\mathbf{v}$ attained in the closed domain $\mathcal{D}$ for any component of $\mathbf{v}$ in $\mathcal{D}$. We have

$$A\mathbf{v}_1 - A\mathbf{v}_2 = \begin{pmatrix} \int_0^x (\Omega(v^1_1 - v^1_2) + \alpha(v^2_1 - v^2_2) + \beta(v^3_1 - v^3_2) + \beta(v^4_1 - v^4_2))\, dx \\ \int_L^x (\alpha(v^1_1 - v^1_2) + \Omega(v^2_1 - v^2_2) + \beta(v^3_1 - v^3_2) + \beta(v^4_1 - v^4_2))\, dx \\ \int_0^y (\beta(v^1_1 - v^1_2) + \beta(v^2_1 - v^2_2) + \Omega(v^3_1 - v^3_2) + \alpha(v^4_1 - v^4_2))\, dy \\ \int_H^y (\beta(v^1_1 - v^1_2) + \beta(v^2_1 - v^2_2) + \alpha(v^3_1 - v^3_2) + \Omega(v^4_1 - v^4_2))\, dy \end{pmatrix}$$

Taking the absolute value of each component we obtain

$$|A\mathbf{v}_1 - A\mathbf{v}_2|(x,y) \leq \begin{pmatrix} x \\ L-x \\ y \\ H-y \end{pmatrix} M\|\mathbf{v}_1 - \mathbf{v}_2\|$$

Where $M = |\Omega| + |\alpha| + |2\beta|$. Hence

$$|A^2\mathbf{v}_1 - A^2\mathbf{v}_2|(x,y) \leq \begin{pmatrix} \frac{x^2}{2} \\ \frac{(L-x)^2}{2} \\ \frac{y^2}{2} \\ \frac{(H-y)^2}{2} \end{pmatrix} M^2\|\mathbf{v}_1 - \mathbf{v}_2\|$$

And finally

$$|A^n\mathbf{v}_1 - A^n\mathbf{v}_2|(x,y) \leq \begin{pmatrix} \frac{x^n}{n!} \\ \frac{(L-x)^n}{n!} \\ \frac{y^n}{n!} \\ \frac{(H-y)^n}{n!} \end{pmatrix} M^n\|\mathbf{v}_1 - \mathbf{v}_2\|$$

For any value of M, there exists a number N such that

$$\|A^N\mathbf{v}_1 - A^N\mathbf{v}_2\| \leq \theta\|\mathbf{v}_1 - \mathbf{v}_2\|, \qquad \theta < 1$$

Hence, the map A^N is contraction and as A is a continuous map the solution of $A\mathbf{v} = \mathbf{v}$ exists and unique. ■

The previous result can be easily generalized to the nonlinear problem

$$i\frac{\partial u^1}{\partial x} + F^1(x,y,\mathbf{u}) = 0, \tag{4.7}$$

$$-i\frac{\partial u^2}{\partial x} + F^2(x,y,\mathbf{u}) = 0, \tag{4.8}$$

$$i\frac{\partial u^3}{\partial y} + F^3(x,y,\mathbf{u}) = 0, \tag{4.9}$$

$$-i\frac{\partial u^4}{\partial y} + F^4(x,y,\mathbf{u}) = 0. \tag{4.10}$$

defined on the rectangle,

$$\mathcal{D} = \{(x, y) : \ 0 \le x \le L, \ 0 \le y \le H\}, \tag{4.11}$$

with the boundary conditions:

$$\begin{aligned} u^1(0, y) = u^1(y), \quad u^2(L, y) = u^2(y), \\ u^3(x, 0) = u^3(x), \quad u^4(x, H) = u^4(x), \end{aligned} \tag{4.12}$$

Theorem 4.2 *Let $u^1(y), u^2(y), u^3(x), u^4(x)$ be continuous and $\mathbf{F}(x, y, \mathbf{u})$ is continuous and satisfy Lipschitz condition in it's "functional" argument*

$$\|\mathbf{F}(x, y; \mathbf{u}_1) - \mathbf{F}(x, y; \mathbf{u}_2)\| \le M\|\mathbf{u}_1 - \mathbf{u}_2\|$$

Then, there exists a unique solution of the the problem (4.7)–(4.12).

Proof. The proof essentially repeats the one for the linear case. The nonlinear system is equivalent to

$$\begin{aligned} u^1(x, y) &= u^1(0, y) + \int_0^x F^1(x, y; \mathbf{u})\, dx \\ u^2(x, y) &= u^2(L, y) + \int_L^x F^2(x, y; \mathbf{u})\, dx \\ u^3(x, y) &= u^3(x, 0) + \int_0^y F^3(x, y; \mathbf{u})\, dy \\ u^4(x, y) &= u^4(x, H) + \int_H^y F^4(x, y; \mathbf{u})\, dy \end{aligned}$$

Setting $\mathbf{w} = (u^1(0, y), u^2(L, y), u^3(x, 0), u^4(x, H))^T$ and defining the integral map A as

$$A\mathbf{u} = \begin{pmatrix} w^1 + \int_0^x F^1(x, y; \mathbf{u})\, dx \\ w^2 + \int_L^x F^2(x, y; \mathbf{u})\, dx \\ w^3 + \int_0^y F^3(x, y; \mathbf{u})\, dy \\ w^4 + \int_H^y F^4(x, y; \mathbf{u})\, dy \end{pmatrix}$$

we find that

$$|A\mathbf{u}_1 - A\mathbf{u}_2|(x,y) \leq \begin{pmatrix} |\int_0^x (F^1(x,y;\mathbf{u}_1) - F^1(x,y;\mathbf{u}_2))\,dx| \\ |\int_L^x (F^2(x,y;\mathbf{u}_1) - F^2(x,y;\mathbf{u}_2)\,dx| \\ |\int_0^y (F^3(x,y;\mathbf{u}_1) - F^3(x,y;\mathbf{u}_2)\,dy| \\ |\int_H^y F^4(x,y;\mathbf{u}_1) - F^4(x,y;\mathbf{u}_2))\,dy| \end{pmatrix} \leq \begin{pmatrix} x \\ L-x \\ y \\ H-y \end{pmatrix} M\|\mathbf{u}_1 - \mathbf{u}_2\|$$

Hence,

$$|A^n\mathbf{u}_1 - A^n\mathbf{u}_2|(x,y) \leq \begin{pmatrix} \frac{x^n}{n!} \\ \frac{(L-x)^n}{n!} \\ \frac{y^n}{n!} \\ \frac{(H-y)^n}{n!} \end{pmatrix} M^n\|\mathbf{u}_1 - \mathbf{u}_2\|$$

and A^n is a contraction map. ■

It is clear that under inclusion of the cubic Kerr nonlinearities into the Maxwell equations (2.1), i.e by decomposition of the refractive index $n = n(\mathbf{x}, |\mathbf{E}|^2)$ into the linear and nonlinear parts [SS]:

$$n(\mathbf{x}, |\mathbf{E}|^2) = n_0 + \epsilon n_1(\mathbf{x}) + \epsilon n_2(\mathbf{x})|\mathbf{E}|^2,$$

the vector function $\mathbf{F}(x,y;\mathbf{u})$ in the coupled-mode system is the sum of linear and cubic terms of u^k and $\bar{u}^k$. The set of admissible vector functions in the statements and proofs of both theorems is the set of continuous vector functions on $\mathcal{D}$, and thus there is no upper bound for $\|\mathbf{u}\|$ and Kerr nonlinearity is not Lipschitz in its functional argument. We can obtain the existence and uniqueness result by restricting the set of admissible vector functions to bounded (in the maximum norm) by the doubled norm of the boundary data $2\|\mathbf{w}\|$ and continuous on $\mathcal{D}$ and considering small enough $\mathcal{D}$ so that the map $A\mathbf{u}$ gives us again an admissible vector function.

Theorem 4.3 *Let $u^1(y), u^2(y), u^3(x), u^4(x)$ be continuous and $\mathbf{F}(\mathbf{u})$ be the sum of linear and cubic terms of u^k and $\bar{u}^k$ representing cubic Kerr nonlinearity and*

$$\max(L,H)(2a + 8b\|\mathbf{w}\|^2) \leq 1$$

where constants a, b are the sums of absolute values of coefficients of $\mathbf{F}$ *in linear and cubic parts correspondingly. Then, there exists a unique solution of the the problem (4.7)–(4.12).*

Proof. We denote $\mathbf{w} = (u^1(y), u^2(y), u^3(x), u^4(x))^T$ and restrict the set of admissible vector functions $\mathbf{u}$, such that $\mathbf{u}$ is continuous on $\mathcal{D}$ and $\|\mathbf{u}\| \leq 2\|\mathbf{w}\|$. Defining the integral map A as

$$A\mathbf{u} = \begin{pmatrix} w^1 + \int_0^x F^1(\mathbf{u})\,dx \\ w^2 + \int_L^x F^2(\mathbf{u})\,dx \\ w^3 + \int_0^y F^3(\mathbf{u})\,dy \\ w^4 + \int_H^y F^4(\mathbf{u})\,dy \end{pmatrix}$$

we find that

$$\|A\mathbf{u}\| \leq \|\mathbf{w}\| + a\max(L,H)\|\mathbf{u}\| + b\max(L,H)\|\mathbf{u}\|^3,$$

where a, b are the sums of absolute values of coefficients of $\mathbf{F}$ in linear and cubic parts correspondingly. Under condition that

$$\max(L,H)(2a + 8b\|\mathbf{w}\|^2) \leq 1$$

the set of admissible functions is mapped by A into itself. As vector function $F(\mathbf{u})$ is Lipschitz on the set of admissible functions and the equation $\mathbf{u} = A\mathbf{u}$ has only one solution. ■

Thus, for the finite norm boundary data there is always a unique solution of the Kerr nonlinear boundary-value problem given that domain is small enough.

4.2 Existence and uniqueness of solution for N waves

Let us consider now the case of N waves in resonance. The characteristic coordinates are introduced from the set of resonant wave vectors

$$\frac{\partial}{\partial \xi^j} = \frac{\mathbf{k}_{j,x}}{k}\frac{\partial}{\partial X} + \frac{\mathbf{k}_{j,y}}{k}\frac{\partial}{\partial Y} + \frac{\mathbf{k}_{j,z}}{k}\frac{\partial}{\partial Z}, \qquad j = 1, \ldots, N,$$

such that characteristic lines are taken in the direction of wave vectors k_j's.

We will consider now two dimensional spatial space $\mathbf{X} = (X, Y)$ for simplicity. The only parallel resonant waves allowed in crystal are counter propagating waves: vectors $(k_{i,x}, k_{i,y})$ and $(k_{j,x}, k_{j,y})$ could be in the opposite directions but any other vector $(k_{l,x}, k_{l,y})$ should be linearly independent of them. Hence, generally characteristics fill the whole plane.

We consider now the general problem of N-wave resonant propagation in the convex crystal. Due to convexity the characteristics for any point inside the domain lie entirely in the domain. Clearly the same family of characteristics can intersect more than one face of the crystal as shown on the Figures 4.2,4.3. As can be seen from the Figure 4.1, we only needed one wave profile at each face.

We consider the following boundary conditions: on avery face of the crystal we give a profile $A'^i(x, y)$ of the wave A^i whose characteristics incidents on the face, we require the continuity of profile on the verges (edges for 3D).

The boundary-value problem for the stationary transmission can be written in the form

$$\frac{\partial a^i}{\partial \xi^i} + F^i(x, y; \mathbf{a}) = 0, \qquad i = 1, \ldots, N \tag{4.13}$$

in the given convex domain $\mathcal{D}$, with the boundary conditions described above, such that profiles $a'^i(x, y)$ are continuous (on the verges as well as on the faces) and

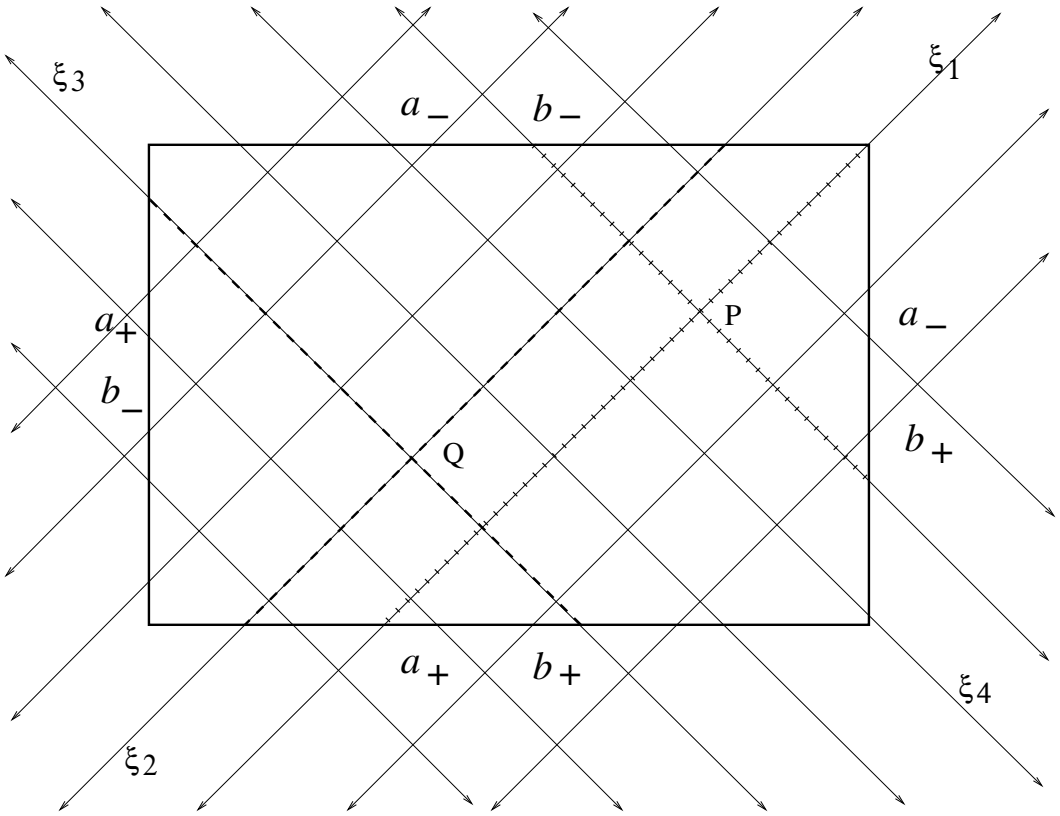

Figure 4.2: Modified boundary value problem for four counter-propagating waves on the plane. The direction of the characteristics is shown with the arrowed lines. The characteristics that are going through points P and Q are shown with dashed lines. The wave a_+ propagates along ξ_1, a_- along ξ_2, b_+ along ξ_3 and b_- along ξ_4. The boundary data for this particular geometry of domain $\mathcal{D}$ is shown.

$\mathbf{F}(x, y, \mathbf{a})$ is continuous and satisfy Lipschitz condition in it's "functional" argument

$$\|\mathbf{F}(x, y; \mathbf{a}_1) - \mathbf{F}(x, y; \mathbf{a}_2)\| \leq M\|\mathbf{a}_1 - \mathbf{a}_2\|$$

Theorem 4.4 *The general transmission problem (4.13) has a unique solution.*

Proof. The proof essentially repeats the one for the four counter-propagating waves. For any point (x, y) in the domain $\mathcal{D}$ we find the N characteristics going through it, we parametrize all characteristics so that $\xi_i = 0$ on the boundary of the domain from which the characteristic goes inside the domain. For the convex domain $\mathcal{D}$ the

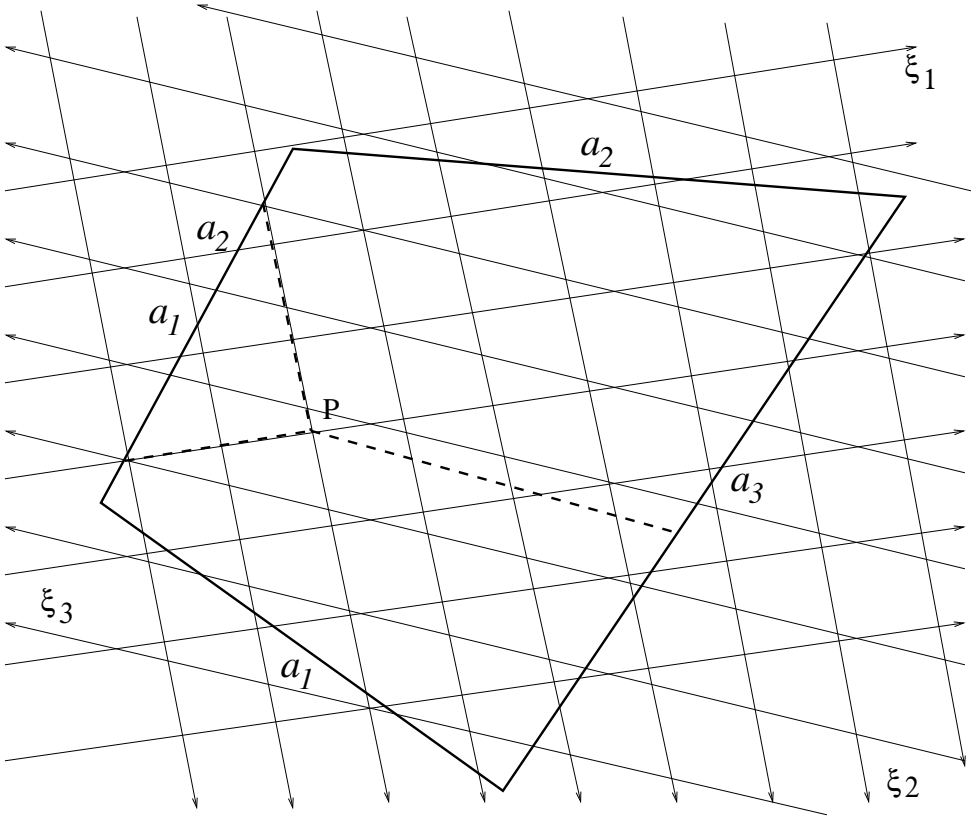

Figure 4.3: The case of three non-parallel families of characteristics. The boundary data for this particular geometry of domain is shown.

nonlinear system is equivalent to

$$a^i(x,y) = a'^i(x(0),y(0)) + \int_0^{\xi^i} F^i(x(\xi^i),y(\xi^i);\mathbf{a})\,d\xi^i, \qquad i = 1,\ldots.N,$$

where integrals are taken along characteristics. Setting $b^i = a'^i(x,y)$ we define the integral map A as

$$A\mathbf{a} = \begin{pmatrix} b^1(x(0),y(0)) + \int_0^{\xi^i} F^1(x(\xi^1),y(\xi^1);\mathbf{a})\,d\xi^1 \\ \vdots \\ b^N(x(0),y(0)) + \int_0^{\xi^N} F^N(x(\xi^N),y(\xi^N);\mathbf{a})\,d\xi^N \end{pmatrix}$$

we find that

$$|A\mathbf{a}_1 - A\mathbf{a}_2| \leq \begin{pmatrix} |\int_0^{\xi^1} (F^1(x,y;\mathbf{a}_1) - F^1(x,y;\mathbf{a}_2))\, d\xi^1| \\ \vdots \\ |\int_0^{\xi^N} (F^N(x,y;\mathbf{a}_1) - F^N(x,y;\mathbf{a}_2))\, d\xi^N| \end{pmatrix}$$

$$\leq \begin{pmatrix} |\int_0^{\xi^1} d\xi^1| \\ \vdots \\ |\int_0^{\xi^N} d\xi^N| \end{pmatrix} M\|\mathbf{a}_1 - \mathbf{a}_2\|$$

$$\leq \begin{pmatrix} \xi^1 \\ \vdots \\ \xi^N \end{pmatrix} M\|\mathbf{a}_1 - \mathbf{a}_2\|$$

Hence,

$$|A^n\mathbf{a}_1 - A^n\mathbf{a}_2| \leq \begin{pmatrix} \frac{(\xi^1)^n}{n!} \\ \vdots \\ \frac{(\xi^N)^n}{n!} \end{pmatrix} M^n\|\mathbf{a}_1 - \mathbf{a}_2\|$$

and A^n is a contraction map. Hence, the equation $A\mathbf{a} = \mathbf{a}$ has a unique solution. ■

The theorems proved can be used for numerical solutions of the coupled-mode systems through iteration of the integral map $\mathbf{u}_{n+1} = A\mathbf{u}_n$. The analytical solutions for linear case is obtained in the next chapter.

4.3 Multi-symplectic structure of the coupled-mode equations

Following [Br], a multi-symplectic system on the plane in canonical form in real coordinates is

$$M\mathbf{u}_x + K\mathbf{u}_y = \nabla h(\mathbf{u}), \qquad \mathbf{u} \in \mathbb{R}^{2n},$$

where M and K are any $2n \times 2n$ skew-symmetric matrices.

An important part of the theory of conservative systems is the Noether theory that relates symmetries and conservation laws. When a conservative system has a Hamiltonian structure the symplectic operator gives a natural correspondence between symmetries and invariants or conserved densities ([O]). However in the classical setting there is only one symplectic operator and therefore there is no relation between symplecticity and the fluxes of a conservation law. In the multi-symplectic framework such a connection is possible and leads to a new and useful decomposition of the Noether theory.

In its simplest setting, finite-dimensional Hamiltonian systems, the connection between symmetry and conservation laws can be stated as follows. Suppose $\mathbf{u} \in \mathbb{R}^{2n}$ and

$$J\mathbf{u}_t = \nabla h(\mathbf{u})$$

with J the usual unit symplectic operator on $\mathbb{R}^{2n}$

$$\begin{pmatrix} 0 & -I_n \\ I_n & 0 \end{pmatrix}$$

Suppose there exists a one-parameter Lie group $G(\epsilon)$ acting symplectically on $\mathbb{R}^{2n}$ which leaves the Hamiltonian functional invariant. Let

$$\mathbf{v} = \frac{d}{d\epsilon}[G(\epsilon)\mathbf{u}]\Big|_{\epsilon=0}$$

and suppose

$$J\mathbf{v} = \nabla p(\mathbf{u}) \tag{4.14}$$

for some functional $p(\mathbf{u})$. Then $\partial_t p = 0$. A proof of this result is given in [O]. The above result connects the action of the symmetry group with the conserved densities but in the case of classical Hamiltonian system it does not establish a connection

between the action of the symmetry and the fluxes. In the expression (4.14) it is the action of the symplectic operator, on the infinitesimal action of the Lie group, that generates the gradient of the conserved quantity. Therefore its generalization to include fluxes is clear: act on V with each element in the family of skew-symmetric operators in the multi-symplectic structure to obtain all the components of the conservation law. This leads to a new decomposition of the Noether theory.

Let $\mathbf{u} \in \mathbb{R}^{2n}$ and consider the multi-symplectic Hamiltonian system

$$M(\mathbf{u})\mathbf{u}_x + K(\mathbf{u})\mathbf{u}_y + L(\mathbf{u})\mathbf{u}_z = \nabla h(\mathbf{u}) \tag{4.15}$$

We say that the system (4.15) is invariant with respect to the action of one parameter Lie group $G(\epsilon)$ if

$$\begin{aligned} h(G(\epsilon)\cdot\mathbf{u}) &= h(\mathbf{u}) \\ DG(\epsilon)^* M(G(\epsilon)\cdot\mathbf{u})DG(\epsilon) &= M(\mathbf{u}) \\ DG(\epsilon)^* K(G(\epsilon)\cdot\mathbf{u})DG(\epsilon) &= K(\mathbf{u}) \\ DG(\epsilon)^* L(G(\epsilon)\cdot\mathbf{u})DG(\epsilon) &= L(\mathbf{u}) \end{aligned} \tag{4.16}$$

where $DG(\epsilon)$ is Jacobian with respect to ϵ and * indicates formal adjoint.

Theorem 4.5 (Bridges, 1997) *Let the Hamiltonian system (4.15) be invariant with respect to the action of a one-parameter Lie group $G(\epsilon)$ with generator $\mathbf{v}$. Suppose there exist a solution $\mathbf{u}(x,y,z)$ and functionals $p(\mathbf{u}), q(\mathbf{u}), r(\mathbf{u})$ such that*

$$M(\mathbf{u})\mathbf{v} = \nabla p(\mathbf{u}), \quad K(\mathbf{u})\mathbf{v} = \nabla q(\mathbf{u}), \quad L(\mathbf{u})\mathbf{v} = \nabla r(\mathbf{u}).$$

Then p, q and r, evaluated at the solution $\mathbf{u}$ of (4.15), satisfy the conservation law

$$\frac{\partial p}{\partial x} + \frac{\partial q}{\partial y} + \frac{\partial r}{\partial z} = 0$$

Proof. The proof of this result is straightforward. Differentiating the first equation of (4.16) with respect to ϵ and setting to zero results in

$$\begin{aligned} 0 = \frac{d}{d\epsilon} h(G(\epsilon)\cdot \mathbf{u})\Big|_{\epsilon=0} &= (\nabla h(\mathbf{u}), \mathbf{v}) \\ &= (M(\mathbf{u})\mathbf{u}_x + K(\mathbf{u})\mathbf{u}_y + L(\mathbf{u})\mathbf{u}_z, \mathbf{v}) \\ = -(\mathbf{u}_x, M(\mathbf{u})\mathbf{v}) - (\mathbf{u}_y, K(\mathbf{u})\mathbf{v}) - (\mathbf{u}_z, L(\mathbf{u})\mathbf{v}) \\ &= -(\mathbf{u}_x, \nabla p) - (\mathbf{u}_y, \nabla q) - (\mathbf{u}_z, \nabla r) \\ &= -\frac{\partial p}{\partial x} - \frac{\partial q}{\partial y} - \frac{\partial r}{\partial z} \end{aligned}$$

proving the claim. ■

We illustrate the multi-symplectic Noether theorem on the example of four counter propagating waves in crystal (4.18)–(4.21).

The system for stationary transmission of four counter-propagating waves can be rewritten in the bi-symplectic Hamiltonian form.

Denoting

$$\begin{aligned} h = \Omega(a_+\overline{a}_+ + a_-\overline{a}_- + b_+\overline{b}_+ + b_-\overline{b}_-) + \alpha(\overline{a}_+a_- + a_+\overline{a}_-) + \alpha(\overline{b}_+b_- + b_+\overline{b}_-) + \\ \beta((b_+ + b_-)(\overline{a}_+ + \overline{a}_-) + (\overline{b}_+ + \overline{b}_-)(a_+ + a_-)) \end{aligned} \tag{4.17}$$

The system becomes

$$\frac{\partial}{\partial x} a_+ = i \frac{\partial h}{\partial \overline{a}_+} \tag{4.18}$$

$$\frac{\partial}{\partial x} a_- = -i \frac{\partial h}{\partial \overline{a}_-} \tag{4.19}$$

$$\frac{\partial}{\partial y} b_+ = i \frac{\partial h}{\partial \overline{b}_+} \tag{4.20}$$

$$\frac{\partial}{\partial y} b_- = -i \frac{\partial h}{\partial \overline{b}_-} \tag{4.21}$$

And corresponding complex conjugate system. Here $a_\pm$, $b_\pm$ and $\overline{a}_\pm$, $\overline{b}_\pm$ are treated as independent variables. Note that first half of the system and it's complex conjugate describes non-autonomous (for some fixed functions $b_\pm$) x-spatial dynamics of (a_+, a_-) with hamiltonian h and the second half of the system and it's complex conjugate describes non-autonomous (for some fixed functions $a_\pm$) y-spatial dynamics of (b_+, b_-) with hamiltonian h.

This system has number of symmetries [PS]

- time inversion

$$a_+ \to \overline{a}_-, a_- \to \bar{a}_+ \tag{4.22}$$

$$b_+ \to \overline{b}_-, b_- \to \bar{b}_+ \tag{4.23}$$

- spatial reflection in x and in y

$$a_+ \to a_-, a_- \to a_+, x \to -x \tag{4.24}$$

$$b_+ \to b_-, b_- \to b_+, y \to -y \tag{4.25}$$

- gauge symmetry

$$(a_+, a_-, b_+, b_-) \mapsto e^{i\phi}(a_+, a_-, b_+, b_-) \tag{4.26}$$

Denoting

$$\mathbf{u} = (\operatorname{Im} a_+, \operatorname{Re} a_-, \operatorname{Re} a_+, \operatorname{Im} a_-, \operatorname{Im} b_+, \operatorname{Re} b_-, \operatorname{Re} b_+, \operatorname{Im} b_-)^T \in \mathbb{R}^8 \tag{4.27}$$

we transfer the system to canonical form

$$\begin{pmatrix} J & 0 \\ 0 & 0 \end{pmatrix} \mathbf{u}_x + \begin{pmatrix} 0 & 0 \\ 0 & J \end{pmatrix} \mathbf{u}_y = \frac{i}{2} \nabla h(\mathbf{u})$$

with J the usual symplectic matrix: $J = \begin{pmatrix} 0 & -I_2 \\ I_2 & 0 \end{pmatrix}$ and $h(\mathbf{u})$ given by (4.17). The group (4.26) obviously conserve symplectic structure M, K, it is a simple rotation in the $\mathbf{u}$ space, therefore, we immediately find the generator (corresponding real parts in vector $\mathbf{u}$ change sign)

$$\mathbf{v} = \begin{pmatrix} u^1 \\ -u^2 \\ -u^3 \\ u^4 \\ \vdots \\ u^8 \end{pmatrix}$$

We have

$$M\mathbf{v} = \begin{pmatrix} u^3 \\ -u^4 \\ u^1 \\ -u^2 \end{pmatrix}$$

which corresponds to $p(\mathbf{u}) = (u^1)^2 - (u^2)^2 + (u^3)^2 - (u^4)^2 = |a_+|^2 - |a_-|^2$ due to (4.27). Similarly $q = |b_+|^2 - |b_-|^2$ and we have conservation law

$$\frac{\partial}{\partial x}\left(|a_+|^2 - |a_-|^2\right) + \frac{\partial}{\partial y}\left(|b_+|^2 - |b_-|^2\right) = 0.$$

We conclude this part with the remark that multi-symplectic structure of the system of four (2D) and six (3D) counter-propagating waves could be very useful in developing numerical algorithms for integrations of such systems, as conservation laws can be used to stabilize numerics (Marsden, Patrick, and Shkoller (1998) **??** - methods derived from descrite variational principle; Bridges and Reich (2001) **??**- methods preserve multi-symplectic conservation law).

Chapter 5

Explicit analytical solution in the linear case

In this chapter we give analytical solutions for some linear coupled-mode systems. We also give an alternative proof of the well-posedness of the boundary-value problem for four counter-propagating waves using the method of separation of variables and generalized Fourier series.

5.1 Transmission of two counter-propagating waves

After separation of variables (4.1), the linear coupled-mode equations (3.8)–(3.9) reduce to the following ODE system:

$$i\frac{da_+}{dZ} + \Omega a_+ + \alpha a_- = 0, \tag{5.1}$$

$$-i\frac{da_-}{dZ} + \alpha a_+ + \Omega a_- = 0. \tag{5.2}$$

The problem (5.1)–(5.2) is defined on the interval $0 \leq Z \leq L_Z$. When the incident wave is illuminated to the photonic crystal from the left, the linear system (5.1)–(5.2) is completed by the boundary conditions:

$$a_+(0) = \alpha_+, \qquad a_-(L_Z) = 0, \tag{5.3}$$

where α_+ is the given amplitude of the incident wave at the left (x, y)-plane of the crystal. The general solution of the ODE system (5.1)–(5.2) is given explicitly as follows:

$$\begin{pmatrix} a_+ \\ a_- \end{pmatrix} = c_+ \begin{pmatrix} \alpha \\ \Omega + i\kappa \end{pmatrix} e^{\kappa Z} + c_- \begin{pmatrix} \alpha \\ \Omega - i\kappa \end{pmatrix} e^{-\kappa Z}, \tag{5.4}$$

where $c_\pm \in \mathbb{C}$ are arbitrary and $\kappa \in \mathbb{C}$ is the root of the determinant equation:

$$\kappa = \sqrt{\alpha^2 - \Omega^2}. \tag{5.5}$$

When $\kappa = iK$, $K \in \mathbb{R}$, the linear dispersion relation $\Omega = \Omega(K)$ follows from the quadratic equation:

$$\Omega^2 = \alpha^2 + K^2. \tag{5.6}$$

The two branches of the dispersion relation (5.6) correspond to the two counter-propagating resonant waves. Their resonance leads to the photonic stop band, which is located in the interval: $|\Omega| < |\alpha|$.

Let $\Omega = 0$ for simplicity, i.e. the detuning frequency is fixed in the middle of the stop band. The unique solution of the boundary-value problem (5.1)–(5.3) follows from the general solution (5.4):

$$\begin{pmatrix} a_+ \\ a_- \end{pmatrix} = \frac{\alpha_+}{\cosh \alpha L_Z} \begin{pmatrix} \cosh \alpha (L_Z - Z) \\ -i \sinh \alpha (L_Z - Z) \end{pmatrix}. \tag{5.7}$$

The transmittance T and reflectance R are defined from the other boundary values of the solution (5.7):

$$T = \left| \frac{a_+(L_Z)}{a_+(0)} \right|^2 = \frac{1}{\cosh^2 \alpha L_Z}, \qquad R = \left| \frac{a_-(0)}{a_+(0)} \right|^2 = \frac{\sinh^2 \alpha L_Z}{\cosh^2 \alpha L_Z},$$

such that the balance identity $T + R = 1$ is satisfied. The analytical solution (5.7) for the two counter-propagating waves is well-known [SS] and is reproduced here for

comparison with the case of four counter-propagating and two oblique waves on the plane.

5.2 Transmission of four counter-propagating waves

The stationary transmission of four counter-propagating waves in the coupled-mode equations (3.12)–(3.15) is studied in the characteristic coordinates (ξ, η):

$$\xi = \frac{X+Y}{2}, \qquad \eta = \frac{X-Y}{2}.$$

After the separation of variables (4.1), the linear coupled-mode equations (3.12)–(3.15) reduce to the PDE system:

$$i\frac{\partial a_+}{\partial \xi} + \Omega a_+ + \alpha a_- + \beta\,(b_+ + b_-) = 0, \tag{5.8}$$

$$-i\frac{\partial a_-}{\partial \xi} + \alpha a_+ + \Omega a_- + \beta\,(b_+ + b_-) = 0, \tag{5.9}$$

$$i\frac{\partial b_+}{\partial \eta} + \beta\,(a_+ + a_-) + \Omega b_+ + \alpha b_- = 0, \tag{5.10}$$

$$-i\frac{\partial b_-}{\partial \eta} + \beta\,(a_+ + a_-) + \alpha b_+ + \Omega b_- = 0. \tag{5.11}$$

The problem (5.8)–(5.11) is defined in a bounded domain on the plane (ξ, η). We consider the rectangle,

$$\mathcal{D} = \{(\xi, \eta) :\ 0 \le \xi \le L_\xi,\ 0 \le \eta \le L_\eta\}, \tag{5.12}$$

which corresponds to a rectangle in physical coordinates (X, Y), rotated at 45° in characteristic coordinates (ξ, η). When the incident wave is illuminated from the left along the main diagonal in the (X, Y)-plane of the photonic crystal, the linear system (5.8)–(5.11) is completed by the boundary conditions:

$$a_+(0,\eta) = \alpha_+(\eta), \qquad a_-(L_\xi, \eta) = 0, \qquad b_+(\xi, 0) = 0, \qquad b_-(\xi, L_\eta) = 0, \tag{5.13}$$

where $\alpha_+(\eta)$ is the given amplitude of the incident wave at the left boundary of the crystal. We give alternative proof of the balance equation for four counter-propagating waves.

Theorem 5.1 *The amplitudes $a_\pm, b_\pm$ of the PDE system (5.8)–(5.11) satisfy the balance equation:*

$$\frac{\partial}{\partial\xi}\left(|a_+|^2-|a_-|^2\right)+\frac{\partial}{\partial\eta}\left(|b_+|^2-|b_-|^2\right)=0. \tag{5.14}$$

Proof. The system (5.8)–(5.11) can be rewritten as follows:

$$i\begin{pmatrix} \frac{\partial}{\partial\xi} & 0 & 0 & 0\\ 0 & -\frac{\partial}{\partial\xi} & 0 & 0\\ 0 & 0 & \frac{\partial}{\partial\eta} & 0\\ 0 & 0 & 0 & -\frac{\partial}{\partial\eta}\end{pmatrix}\begin{pmatrix} a_+\\ a_-\\ b_+\\ b_-\end{pmatrix}+\begin{pmatrix} \Omega & \alpha & \beta & \beta\\ \alpha & \Omega & \beta & \beta\\ \beta & \beta & \Omega & \alpha\\ \beta & \beta & \alpha & \Omega\end{pmatrix}\begin{pmatrix} a_+\\ a_-\\ b_+\\ b_-\end{pmatrix}=0$$

or

$$i\left(\gamma^1\frac{\partial}{\partial\xi}+\gamma^2\frac{\partial}{\partial\eta}\right)\psi+M\psi=0$$

where

$$\gamma^1=\begin{pmatrix} 1 & 0 & 0 & 0\\ 0 & -1 & 0 & 0\\ 0 & 0 & 0 & 0\\ 0 & 0 & 0 & 0\end{pmatrix},\gamma^2=\begin{pmatrix} 0 & 0 & 0 & 0\\ 0 & 0 & 0 & 0\\ 0 & 0 & 1 & 0\\ 0 & 0 & 0 & -1\end{pmatrix},$$

$$M=\begin{pmatrix} \Omega & \alpha & \beta & \beta\\ \alpha & \Omega & \beta & \beta\\ \beta & \beta & \Omega & \alpha\\ \beta & \beta & \alpha & \Omega\end{pmatrix},\psi=\begin{pmatrix} a_+\\ a_-\\ b_+\\ b_-\end{pmatrix}$$

To obtain the balance equation we multiply this system from the left by $\bar{\psi}^T$, multiply the complex conjugate system from the left by ψ^T and subtract the results

$$i\left(\bar{\psi},\gamma^1\frac{\partial}{\partial\xi}\psi\right)+i\left(\psi,\gamma^1\frac{\partial}{\partial\xi}\bar{\psi}\right)+i\left(\bar{\psi},\gamma^2\frac{\partial}{\partial\eta}\psi\right)+i\left(\psi,\gamma^2\frac{\partial}{\partial\eta}\bar{\psi}\right)+\left(\bar{\psi},M\psi\right)-\left(\psi,M\bar{\psi}\right)=0$$

As γ^1 , γ^2 , M are symmetric we get

$$\frac{\partial}{\partial\xi}(\bar{\psi}\gamma^1\psi) + \frac{\partial}{\partial\eta}(\bar{\psi}\gamma^2\psi) = 0$$

Using the degenerate structure of γ^1 , γ^2 we obtain the balance equation

$$\frac{\partial}{\partial\xi}(a_+\bar{a}_+ - a_-\bar{a}_-) + \frac{\partial}{\partial\eta}(b_+\bar{b}_+ - b_-\bar{b}_-) = 0$$

or

$$\frac{\partial}{\partial\xi}\left(|a_+|^2 - |a_-|^2\right) + \frac{\partial}{\partial\eta}\left(|b_+|^2 - |b_-|^2\right) = 0.$$

■

The linear dispersion relation $\Omega = \Omega(K_\xi, K_\eta)$, where (K_ξ, K_η) are Fourier wave numbers, follows from the determinant equation of the linear PDE system (5.8)–(5.11).

Lemma 5.2 *The linear dispersion relation $\Omega = \Omega(K_\xi, K_\eta)$ is defined by roots of $D(\Omega, K_\xi, K_\eta)$, where*

$$D(\Omega, K_\xi, K_\eta) = (\Omega^2 - \alpha^2 - K_\xi^2)(\Omega^2 - \alpha^2 - K_\eta^2) - 4\beta^2(\Omega - \alpha)^2. \tag{5.15}$$

There exists real-valued roots $D(0, K_\xi, K_\eta) = 0$ for $\alpha^2 \le 4\beta^2$, while no roots exist for $\alpha^2 > 4\beta^2$.

Proof. The determinant equation follows from the PDE system (5.8)–(5.11) for the Fourier modes $e^{i(K_\xi\xi + K_\eta\eta)}$ in the explicit form:

$$D(\Omega, K_\xi, K_\eta) = \begin{vmatrix} \Omega - K_\xi & \alpha & \beta & \beta \\ \alpha & \Omega + K_\xi & \beta & \beta \\ \beta & \beta & \Omega - K_\eta & \alpha \\ \beta & \beta & \alpha & \Omega + K_\eta \end{vmatrix}. \tag{5.16}$$

Although the straightforward computations of $D(\Omega, K_\xi, K_\eta)$ are involved technically, it is easy to compute that:

$$\frac{\partial D}{\partial \Omega} = 2\Omega\left(\Omega^2 - \alpha^2 - K_\xi^2\right) + 2\Omega\left(\Omega^2 - \alpha^2 - K_\eta^2\right) - 8\beta^2\Omega + 8\alpha\beta^2 \tag{5.17}$$

and

$$D(0, K_\xi, K_\eta) = (\alpha^2 + K_\xi^2)(\alpha^2 + K_\eta^2) - 4\alpha^2\beta^2. \tag{5.18}$$

Integrating (5.17)–(5.18), we find that $D(\Omega, K_\xi, K_\eta)$ is given by (5.15). When $\alpha^2 > 4\beta^2$ the function $D(0, K_\xi, K_\eta)$ is positive definite on $(K_\xi, K_\eta) \in \mathbb{R}^2$ such that no real-valued roots (K_ξ, K_η) exist for $\Omega = 0$. When $\alpha^2 \leq 4\beta^2$, there exist two curves on the (K_ξ, K_η)-plane, which correspond to the real-valued roots of $D(0, K_\xi, K_\eta)$. ■

There are four surfaces of the dispersion relations $\Omega = \Omega(K_\xi, K_\eta)$, which correspond to the four resonant counter-propagating Bloch waves. When $\alpha^2 > 4\beta^2$, the interaction of four resonant waves leads to the stop band near the zero detuning frequency $\Omega = 0$. When $\alpha^2 \leq 4\beta^2$, no stop bands occur in the interaction of the four resonant waves.

We consider solutions of the system (5.8)–(5.11) at $\Omega = 0$. By separating variables [St], we reduce the PDE problem to two ODE problems as follows:

$$a_+(\xi, \eta) = u_+(\xi)w_a(\eta), \qquad a_-(\xi, \eta) = u_-(\xi)w_a(\eta) \tag{5.19}$$

$$b_+(\xi, \eta) = w_b(\xi)v_+(\eta), \qquad b_-(\xi, \eta) = w_b(\xi)v_-(\eta), \tag{5.20}$$

where

$$v_+(\eta) + v_-(\eta) = \mu w_a(\eta), \qquad u_+(\xi) + u_-(\xi) = -\lambda w_b(\xi),$$

parameters (λ, μ) are arbitrary, and vectors $(u_+, u_-)^T$ and $(v_+, v_-)^T$ solve the two uncoupled ODE systems:

$$\begin{pmatrix} i\partial_\xi & \alpha \\ \alpha & -i\partial_\xi \end{pmatrix} \begin{pmatrix} u_+ \\ u_- \end{pmatrix} = \beta\Gamma^{-1} \begin{pmatrix} 1 & 1 \\ 1 & 1 \end{pmatrix} \begin{pmatrix} u_+ \\ u_- \end{pmatrix} \tag{5.21}$$

and

$$\begin{pmatrix} i\partial_\eta & \alpha \\ \alpha & -i\partial_\eta \end{pmatrix} \begin{pmatrix} v_+ \\ v_- \end{pmatrix} = \beta\Gamma \begin{pmatrix} 1 & 1 \\ 1 & 1 \end{pmatrix} \begin{pmatrix} v_+ \\ v_- \end{pmatrix}, \tag{5.22}$$

where $\Gamma = \lambda/\mu$. The boundary conditions for (5.21)–(5.22) follow from (5.13) as follows:

$$u_+(0) = 1, \qquad u_-(L_\xi) = 0, \tag{5.23}$$

and

$$v_+(0) = v_-(L_\eta) = 0. \tag{5.24}$$

The homogeneous problem (5.22) and (5.24) defines the spectrum of Γ, while the inhomogeneous problem (5.21) and (5.23) defines a unique particular solution (5.19)–(5.20). The general solution of the problem (5.8)–(5.11) with the boundary values (5.13) is thought to be a linear superposition of infinitely many particular solutions, if the convergence and completeness of the decomposition formulas can be proved [St]. We first give solutions of the two problems above and then consider the orthogonality and completeness of the generalized Fourier series.

Lemma 5.3 *All eigenvalues Γ of the homogeneous problem (5.22) and (5.24) are given by non-zero roots of the characteristic equation:*

$$\mathcal{R} = \left\{ k \in \mathbb{C} : \left(\frac{k-\alpha}{k+\alpha} \right)^2 e^{-2ikL_\eta} = 1,\ \mathrm{Re}(k) \geq 0,\ k \neq 0 \right\}, \tag{5.25}$$

such that

$$\Gamma = \frac{\alpha^2 + k^2}{2\alpha\beta}. \tag{5.26}$$

Let $\alpha > 0$. Then, the roots $k \in \mathcal{R}$ are all located in the first open quadrant of $k \in \mathbb{C}$. Moreover, all roots are simple and there exists $C > 0$ and $N \in \mathcal{N}$ such that only one root $k \in \mathcal{R}$ is located in each rectangle:

$$\mathcal{D}_n^+ = \left\{ k \in \mathbb{C} : \ \frac{\pi(4n-1)}{2L_\eta} < k < \frac{\pi(4n+1)}{2L_\eta}, \ 0 < \text{Im}(k) < C \right\}, \qquad n \geq N$$

and

$$\mathcal{D}_n^- = \left\{ k \in \mathbb{C} : \ \frac{\pi(4n+1)}{2L_\eta} < k < \frac{\pi(4n+3)}{2L_\eta}, \ 0 < \text{Im}(k) < C \right\}, \qquad n \geq N.$$

Proof. The general solution of the ODE system (5.22) with the use of (5.26) is found explicitly as follows:

$$\begin{pmatrix} v_+ \\ v_- \end{pmatrix} = c_k \begin{pmatrix} \alpha - k \\ \alpha + k \end{pmatrix} e^{ik\eta} + c_{-k} \begin{pmatrix} \alpha + k \\ \alpha - k \end{pmatrix} e^{-ik\eta}. \tag{5.27}$$

The coefficients c_k and c_{-k} satisfy the relations due to the boundary conditions (5.24):

$$\frac{c_k}{c_{-k}} = \frac{k+\alpha}{k-\alpha} = \frac{k-\alpha}{k+\alpha} e^{-2ikL_\eta}, \tag{5.28}$$

from which the characteristic equation (5.25) for roots $k \in \mathbb{C}$ follows. The symmetric roots k and $(-k)$ correspond to the same Γ and $v_\pm(\eta)$. The root $k = 0$ corresponds to the zero solution for $v_\pm(\eta)$. Therefore, the roots $k = 0$ and $\text{Re}(k) \leq 0$ are excluded from the definition of $\mathcal{R}$. The characteristic equation (5.25) is equivalent to the modulus equation:

$$\frac{|k-\alpha|}{|k+\alpha|} = \left| e^{ikL_\eta} \right|.$$

When $\alpha > 0$, the left-hand-side equals to one at $\text{Re}(k) = 0$ and is smaller than one for $\text{Re}(k) > 0$. The right-hand-side equals to one at $\text{Im}(k) = 0$ and is larger than one for $\text{Im}(k) < 0$. Therefore, roots $k \in \mathcal{R}$ may only occur in the first open quadrant of $k \in \mathbb{C}$.

All roots $k \in \mathcal{R}$ are simple, since

$$f'(k) = -\frac{2i(k+\alpha)}{(k-\alpha)} \left[(k^2 - \alpha^2) L_\eta + 2i\alpha \right] \neq 0$$

for $f(k) = (k-\alpha)^2 e^{-2ikL_\eta} - (k+\alpha)^2 = 0$, as the values of $k^2 - \alpha^2$ for $k \in \mathcal{R}$ are located in upper half-plane of the complex plane.

The characteristic equation (5.25) split into two sets of roots $\mathcal{R}_+$ and $\mathcal{R}_-$, such that $\mathcal{R}_+ \cup \mathcal{R}_- = \mathcal{R}$, where

$$\mathcal{R}_\pm = \left\{ k \in \mathbb{C} : \ \frac{k-\alpha}{k+\alpha}\, e^{-ikL_\eta} = \pm 1, \ \mathrm{Re}(k) > 0 \right\}. \tag{5.29}$$

We consider the set $k \in \mathcal{R}_+$ and rewrite it in the form $f(k) = g(k)$, where

$$f(k) = e^{ikL_\eta} - 1, \qquad g(k) = -\frac{2\alpha}{k+\alpha}.$$

The function $f(k)$ has a zero at

$$k = k_n = \frac{2\pi n}{L_\eta}, \qquad n \geq 1.$$

Let us consider the domain

$$\bar{\mathcal{D}}_n^+ = \left\{ k \in \mathbb{C} : \ \frac{\pi(4n-1)}{2L_\eta} < k < \frac{\pi(4n+1)}{2L_\eta}, \ -C < \mathrm{Im}(k) < C \right\}, \qquad n \geq N$$

for some large $C > 0$ and N such that $\frac{\pi(4n-1)}{2L_\eta} > \alpha$, that surrounds a simple zero of $f(k)$ at $k = k_n$. It is clear that for sufficiently large C $|f(k)| > |g(k)|$ on the boundary of $\bar{\mathcal{D}}_n^+$. By the Rouche's Theorem, the function $f(k) + g(k)$ has the same number of zeros inside $\mathcal{D}_n^+$ as $f(k)$ does, i.e. only one zero. We can change $\bar{\mathcal{D}}_n^+$ to $\mathcal{D}_n^+$ as all $k \in \mathcal{R}$ lie in the first open quadrant. The same analysis applies to the second set $k \in \mathcal{R}_-$ in the domain $\mathcal{D}_n^-$. ■

Roots $k \in \mathcal{R}$ and $(-k) \in \mathcal{R}$ are shown on Figure 5.1 from the numerical solution of the characteristic equation (5.25) for $\alpha = 1$ and $L_\eta = 20$. In agreement with Lemma 5.3, all roots $k \in \mathcal{R}$ are isolated points in the first open quadrant, which

accumulate to the real axis of k at infinity. The standard analysis of analytic functions at infinity leads to the asymptotic formula for distribution of large roots k in the domain $|k| > k_0 \gg 1$:

$$(5.30)\; k_n^+ = \frac{2\pi n}{L_\eta} + \frac{i\alpha}{\pi n} + \mathrm{O}\left(\frac{1}{n^2}\right), \quad k_n^- = \frac{\pi(1+2n)}{L_\eta} + \frac{2i\alpha}{\pi(1+2n)} + \mathrm{O}\left(\frac{1}{n^2}\right),$$

where n is large positive integer. The leading order of the asymptotic approximation (5.30) is also shown on Figure 5.1 by dotted curves. The two sets in (5.30) correspond to the splitting $k \in \mathcal{R}_\pm$ in (5.29).

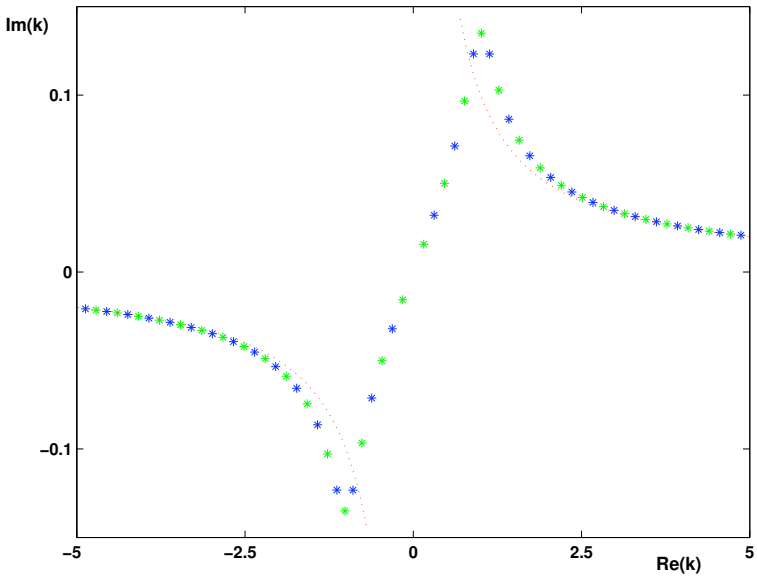

Figure 5.1: Roots $k \in \mathcal{R}$ and $(-k) \in \mathcal{R}$ of the characteristic equation (5.25) for $\alpha = 1$ and $L_\eta = 20$. Dark dots show roots of $\mathcal{R}_+$ and bright dots show roots of $\mathcal{R}_-$. The dotted curves show the leading-order asymptotic approximation (5.30).

The eigenfunction $v(\eta) = v_+(\eta) + v_-(\eta)$ is symmetric (anti-symmetric) with respect to $\eta = L_\eta/2$ for $k \in \mathcal{R}_+$ ($k \in \mathcal{R}_-$). Moreover, explicit formulas for $v(\eta)$ follow

from (5.27) and (5.28):

$$k \in \mathcal{R}_+ : \; v(\eta) = c_+ \cos k \left(\frac{L_\eta}{2} - \eta \right),$$
$$k \in \mathcal{R}_- : \; v(\eta) = c_- \sin k \left(\frac{L_\eta}{2} - \eta \right),$$

where (c_+, c_-) are normalization constants. Asymptotic solutions (5.30) correspond to two sets of eigenfunctions

$$\left\{ \cos(\pi n \tilde{\eta}), \;\; \sin\left(\frac{\pi(2n+1)\tilde{\eta}}{2} \right) \right\}, \qquad \tilde{\eta} = \frac{2\eta}{L_\eta} - 1, \tag{5.31}$$

which solve the homogeneous Neumann's problem on the normalized interval $-1 \leq \tilde{\eta} \leq 1$.

Lemma 5.4 *Let Γ be an eigenvalue of the problem (5.22) and (5.24). There exists a unique solution of the non-homogeneous problem (5.21) and (5.23) for this Γ.*

Proof. A general solution of the ODE system (5.21) is found explicitly as follows:

$$\begin{pmatrix} u_+ \\ u_- \end{pmatrix} = d_k \begin{pmatrix} \alpha^2 + k^2 - 2\beta^2 \\ \lambda_k(\alpha^2 + k^2) + 2\beta^2 \end{pmatrix} e^{i\alpha\lambda_k \eta} + d_{-k} \begin{pmatrix} \alpha^2 + k^2 - 2\beta^2 \\ -\lambda_k(\alpha^2 + k^2) + 2\beta^2 \end{pmatrix} e^{-i\alpha\lambda_k \eta}, \tag{5.32}$$

where

$$\lambda_k = \sqrt{\frac{4\beta^2}{\alpha^2 + k^2} - 1}. \tag{5.33}$$

The relation (5.33) satisfies the determinant equation (5.15), such that $D(0, \alpha\lambda_k, k) = 0$. Using the boundary conditions (5.23), coefficients d_k and d_{-k} are found uniquely, under the constraint:

$$u_0 = \lambda_k(\alpha^2 + k^2) \cos \alpha\lambda_k L_\xi + 2i\beta^2 \sin \alpha\lambda_k L_\xi \neq 0. \tag{5.34}$$

We show that $u_0 \neq 0$. The equation $u_0 = 0$ can be rewritten in the form:

$$\frac{(\lambda_k - 1)^2}{(\lambda_k + 1)^2} = e^{2i\alpha\lambda_k L_\xi}. \tag{5.35}$$

By analysis of Lemma 5.3, it is clear that non-zero roots of the characteristic equation (5.35) may exist only in the first and in the third open quadrant of $\lambda_k \in \mathbb{C}$ for $\alpha > 0$. On the other hand the map $k \to \lambda_k$ given by (5.33) maps first quadrant onto second and third quadrant onto forth one. Thus there could not be a solution of (5.34) except when k is mapped into $\lambda = 0$: $\sqrt{\frac{4\beta^2}{\alpha^2+k^2} - 1} = 0$. In this case $k \in \mathcal{R}$ must be purely real or imaginary which is not the case. Therefore, the relation (5.33) leads to contradiction, which proves that $u_0 \neq 0$. ■

Solutions of the non-homogeneous problem (5.21) and (5.23) with the normalization $u_+(0) = u_0 \neq 0$ can be written explicitly by eliminating d_k and d_{-k} from the implicit form (5.32):

$$\begin{pmatrix} u_+ \\ u_- \end{pmatrix} = \lambda_k(\alpha^2+k^2) \begin{pmatrix} 1 \\ 0 \end{pmatrix} \cos \alpha\lambda_k(L_\xi - \xi) + i \begin{pmatrix} 2\beta^2 \\ \alpha^2 + k^2 - 2\beta^2 \end{pmatrix} \sin \alpha\lambda_k(L_\xi - \xi). \tag{5.36}$$

When the representation (5.19) is used for $\alpha_+(\eta) = a_+(0, \eta)$.

The function $\alpha_+(\eta)$ is expanded as series of scalar eigenfunctions $v(\eta) = v_+(\eta) + v_-(\eta)$, defined for roots $k \in \mathcal{R}$. This decomposition is only possible if the set of eigenfunctions $v(\eta)$ is orthogonal and complete.

Lemma 5.5 *There exists a set of normalized and orthogonal eigenfunctions $v_j(\eta)$ for distinct roots $k = k_j \in \mathcal{R}$, according to the inner product:*

$$\int_0^{L_\eta} v_i(\eta) v_j(\eta) d\eta = \delta_{i,j}. \tag{5.37}$$

Proof. The set of adjoint eigenvectors to the problem (5.22) and (5.24) with respect to the standard inner product in $L^2([0, L_\eta])$ is given by the vectors $(\bar{v}_-, \bar{v}_+)^T$. As a result, the scalar eigenfunctions $v_j(\eta)$ for distinct roots $k = k_j$ satisfy the orthogonality relations (5.37) with $i \neq j$. The scalar eigenfunction $v(\eta)$ is found from (5.27)

and (5.28) in the explicit form:

$$v(\eta) = c_0 \left(k \cos k\eta + i\alpha \sin k\eta\right), \tag{5.38}$$

where c_0 is a normalization constant. Integrating $v^2(\eta)$ on $\eta \in [0, L_\eta]$, we confirm that the eigenfunctions $v_j(\eta)$ can be normalized by the inner product (5.37) with $i = j$, under the constraint:

$$(k^2 - \alpha^2)L_\eta + 2i\alpha \neq 0. \tag{5.39}$$

Since the values of $k^2 - \alpha^2$ for $k \in \mathcal{R}$ are located in upper half-plane of the complex plane, the constraint (5.39) is met for $\alpha > 0$ (constraint (5.39) is the condition that all roots $k \in \mathcal{R}$ are simple). ■

Proposition 5.6 *Any continuously differentiable complex-valued function $f(\eta)$ on $0 \leq \eta \leq L_\eta$ is uniquely represented by the series of eigenfunctions:*

$$f(\eta) = \sum_{\text{all } k_j \in \mathcal{R}} c_j v_j(\eta), \qquad c_j = \int_0^{L_\eta} f(\eta) v_j(\eta) d\eta, \tag{5.40}$$

and the series converges to $f(\eta)$ uniformly on $0 \leq \eta \leq L_\eta$.

Proof. It follows from (5.22) and (5.24) that the scalar eigenfunction $v(\eta)$ solves the second-order boundary-value problem:

$$v'' + k^2 v = 0, \tag{5.41}$$

such that

$$iv'(0) + \alpha v(0) = 0, \qquad -iv'(L_\eta) + \alpha v(L_\eta) = 0. \tag{5.42}$$

The Sommerfeld radiation boundary conditions (5.42) explain why the spectrum of the formally self-adjoint operator (5.41) is complex-valued. The statement of Proposition follows from Expansion Theorem [CL, p.303], since the theorem's condition is

satisfied: $A_{2,4} = 1$, where $A_{2,4}$ is the determinant of the second and fourth columns of the matrix A, associated with the boundary conditions:

$$A = \begin{pmatrix} \alpha & i & 0 & 0 \\ 0 & 0 & \alpha & -i \end{pmatrix}.$$

The key idea here is that asymptotically the eigenvalue problem is the homogeneous Neumann's problem. As a result, the Fourier series of asymptotic eigenfunctions (5.31) approximates the series expansion (5.40) for large roots $k = k_n^{\pm}$ uniformly on $\eta \in [0, L_\eta]$. The uniform convergence of (5.40) follows from that of the Fourier series [St]. ■

Using separation of variables and convergence of series of eigenfunctions, we summarize the existence and uniqueness results on the generalized Fourier series solutions of the linear boundary-value problem (5.8)–(5.11) and (5.13) with $\Omega = 0$.

Proposition 5.7 *Let the set $\{c_j\}$ be uniquely defined by the series (5.40) for $f(\eta) = \alpha_+(\eta)$. There exists a unique continuously differentiable solution of the boundary-value problem (5.8)–(5.11) and (5.13) with $\Omega = 0$ in the domain (5.12):*

$$a_+(\xi,\eta) = \sum_{\text{all } k_j \in \mathcal{R}} c_j \frac{u_{+j}(\xi)}{u_{+j}(0)} \left(v_{+j}(\eta) + v_{-j}(\eta)\right), \tag{5.43}$$

$$a_-(\xi,\eta) = \sum_{\text{all } k_j \in \mathcal{R}} c_j \frac{u_{-j}(\xi)}{u_{+j}(0)} \left(v_{+j}(\eta) + v_{-j}(\eta)\right), \tag{5.44}$$

$$b_+(\xi,\eta) = -\sum_{\text{all } k_j \in \mathcal{R}} c_j \frac{u_{+j}(\xi) + u_{-j}(\xi)}{\Gamma_j u_{+j}(0)} v_{+j}(\eta), \tag{5.45}$$

$$b_-(\xi,\eta) = -\sum_{\text{all } k_j \in \mathcal{R}} c_j \frac{u_{+j}(\xi) + u_{-j}(\xi)}{\Gamma_j u_{+j}(0)} v_{-j}(\eta). \tag{5.46}$$

We illustrate the generalized Fourier series solutions (5.43)–(5.46) with two examples: (i) a single term of the generalized Fourier series and (ii) a constant input function $\alpha_+(\eta) = \alpha_+$. For both examples, we compute the integral invariants for

the incident ($\mathcal{I}_{\rm in}$), transmitted ($\mathcal{I}_{\rm out}$), reflected ($\mathcal{I}_{\rm ref}$) and diffracted ($\mathcal{I}_{\rm dif}$) waves from their definitions:

$$\begin{aligned} \mathcal{I}_{\rm in} &= \int_0^{L_\eta} |a_+(0,\eta)|^2 d\eta, \qquad \mathcal{I}_{\rm out} = \int_0^{L_\eta} |a_+(L_\xi,\eta)|^2 d\eta, \\ \mathcal{I}_{\rm ref} &= \int_0^{L_\eta} |a_-(0,\eta)|^2 d\eta, \qquad \mathcal{I}_{\rm dif} = \int_0^{L_\xi} \left(|b_+(\xi,L_\eta)|^2 + |b_-(\xi,0)|^2 \right) d\xi. \end{aligned}$$

Let the transmittance T, reflectance R and diffractance D be defined from the relations:

$$T = \frac{\mathcal{I}_{\rm out}}{\mathcal{I}_{\rm in}}, \qquad R = \frac{\mathcal{I}_{\rm ref}}{\mathcal{I}_{\rm in}}, \qquad D = \frac{\mathcal{I}_{\rm dif}}{\mathcal{I}_{\rm in}}.$$

The integral invariants satisfy the balance identity:

$$R + T + D = 1,$$

which follows from integration of the balance equation:

$$\frac{\partial}{\partial \xi} \left(|a_+|^2 - |a_-|^2 \right) + \frac{\partial}{\partial \eta} \left(|b_+|^2 - |b_-|^2 \right) = 0.$$

First, we consider a single term of the Fourier series solutions (5.43)–(5.46). The transmittance and reflectance for $k \in \mathcal{R}$ are found from (5.36) in the explicit form:

$$\begin{aligned} T_k &= \left| \frac{\lambda_k(\alpha^2+k^2)}{\lambda_k(\alpha^2+k^2)\cos\alpha\lambda_k L_\xi + 2i\beta^2 \sin\alpha\lambda_k L_\xi} \right|^2, \\ R_k &= \left| \frac{(\alpha^2+k^2-2\beta^2)\sin\alpha\lambda_k L_\xi}{\lambda_k(\alpha^2+k^2)\cos\alpha\lambda_k L_\xi + 2i\beta^2 \sin\alpha\lambda_k L_\xi} \right|^2, \end{aligned}$$

while the diffractance is found from the balance identity as $D_k = 1 - T_k - R_k$. These integral invariants of the stationary transmission for $\alpha = 1$ and $L_\xi = L_\eta = 20$ are shown on Figure 5.2 for $\beta = 0.25$ and on Figure 5.3 for $\beta = 0.75$. In the first case, when $\alpha^2 > 4\beta^2$, there is a stop band at $\Omega = 0$, such that all modes are fully reflected, except for small losses due to diffraction. In the second case, when $\alpha^2 < 4\beta^2$, there is no stop band at $\Omega = 0$, such that transmittance and diffractance are large for smaller values of $|k|$ and become negligible for larger values of $|k|$.

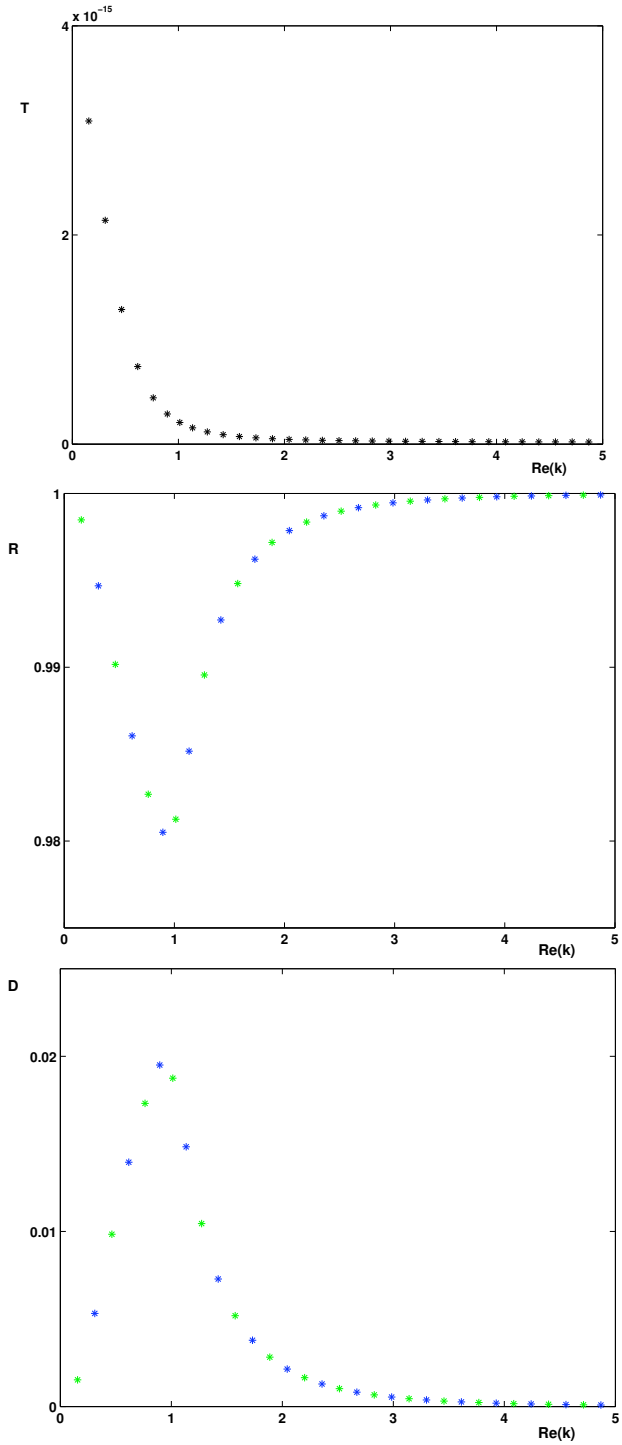

Figure 5.2: Transmittance (T_k), reflectance (R_k), and diffractance (D_k) versus Re(k) for the roots $k \in \mathcal{R}$, when $\alpha = 1$, $\beta = 0.25$, and $L_\xi = L_\eta = 20$.

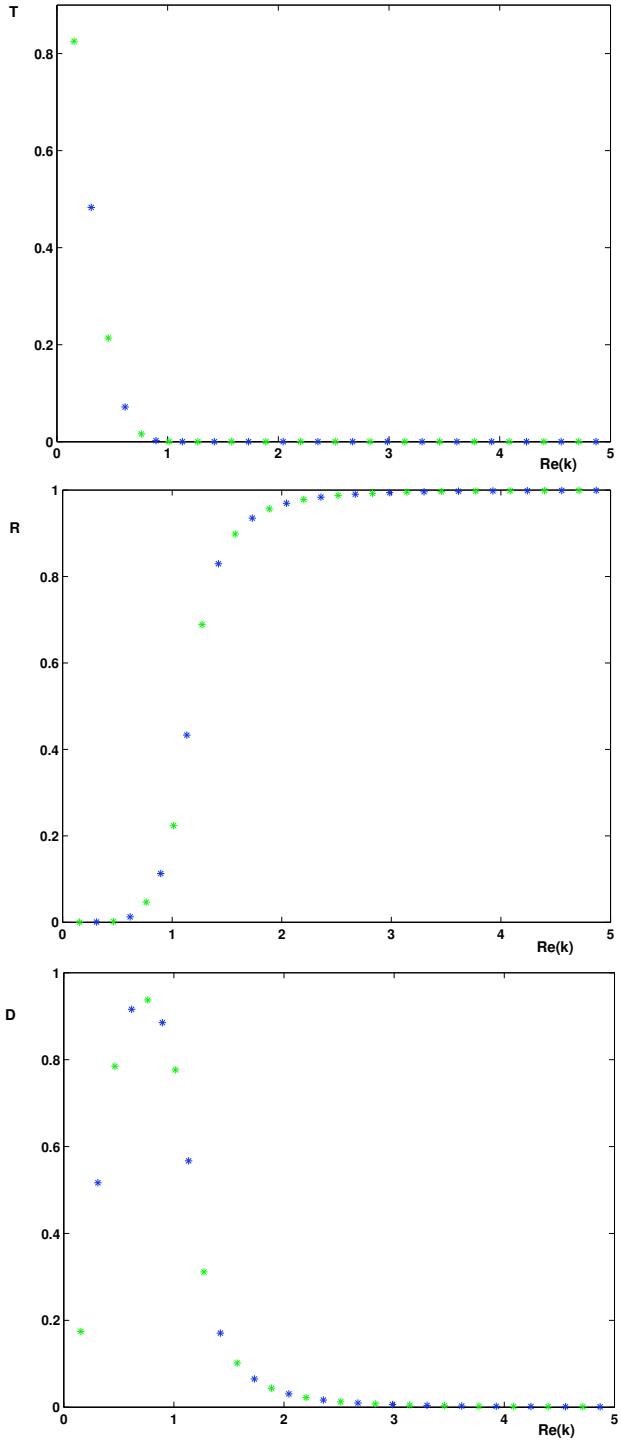

Figure 5.3: Transmittance (T_k), reflectance (R_k), and diffractance (D_k) versus Re(k) for the roots $k \in \mathcal{R}$, when $\alpha = 1$, $\beta = 0.75$, and $L_\xi = L_\eta = 20$.

Next, we consider a constant input function:

$$\alpha_+(\eta) = \alpha_+, \qquad \eta \in [0, L_\eta], \tag{5.47}$$

when c_j can be found from (5.40):

$$c_j = \frac{4i\alpha\alpha_+}{k_j[L(k_j^2 - \alpha^2) + 2i\alpha]}, \qquad k_j \in \mathcal{R}_+,$$

and $c_j = 0$ for $k_j \in \mathcal{R}_-$. The solution surfaces $|a_\pm(\xi, \eta)|^2$ and $|b_\pm(\xi, \eta)|^2$ in the domain (5.12) are shown for $\alpha = 1$, $L_\xi = L_\eta = 20$, and $\alpha_+ = 1$ on Figure 5.4 for $\beta = 0.25$ and on Figure 5.5 for $\beta = 0.75$. We can see from the figures that the boundary conditions (5.13) and (5.47) are satisfied by the truncated generalized Fourier series (5.43)–(5.46) with only 30 first terms.

Parseval's identity can not be applied to eigenfunctions $v_j(\eta)$, because the inner product (5.37) is not the standard inner product in $L^2([0, L_\eta])$. As a result, the energy spectrum of $I_{\rm out}$, $I_{\rm ref}$, and $I_{\rm dif}$ can not be decomposed into a superposition of the squared amplitudes $|c_j|^2$. Nevertheless, the numerical values for T, R, and D can be found from numerical integration of the solution surfaces (5.47)–(5.47). The numerical values are

$$\beta = 0.25: \quad T \approx 3 \times 10^{-15}, \quad R \approx 0.9853, \quad D \approx 0.0147,$$

$$\beta = 0.75: \quad T \approx 0.7394, \quad R \approx 0.0133, \quad D \approx 0.2473,$$

such that $T + R + D \approx 1$. When $\alpha^2 > 4\beta^2$, there exists a stop band at $\Omega = 0$ and the incident wave is reflected from the photonic crystal with energy loss of 1.5% due to diffraction. When $\alpha^2 < 4\beta^2$, there is no stop band at $\Omega = 0$ and the incident wave is transmitted along the photonic crystal with energy loss of 26% due to reflection and diffraction.

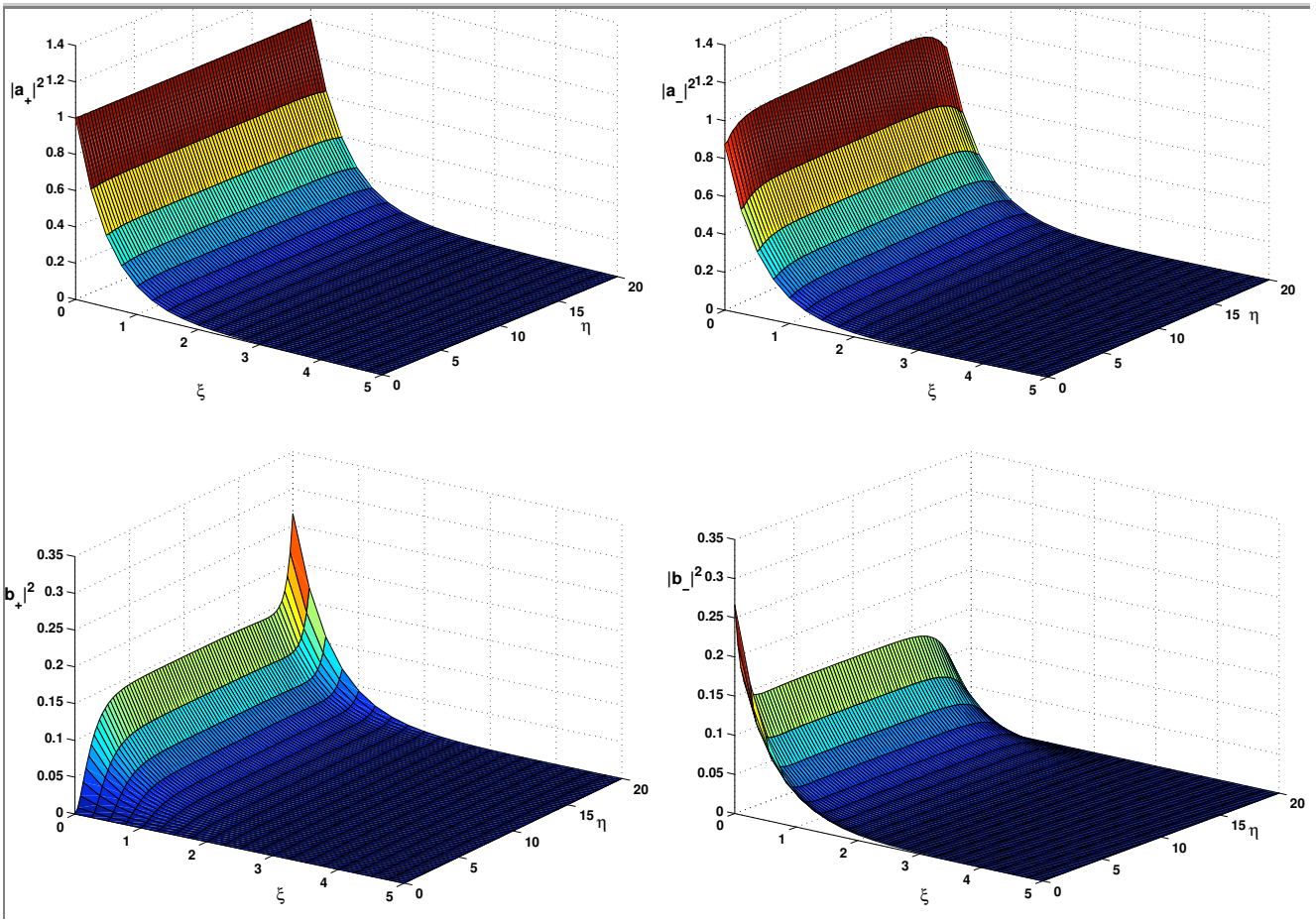

Figure 5.4: Solution surfaces $|a_{\pm}|^2(\xi,\eta)$ and $|b_{\pm}|^2(\xi,\eta)$ on the domain (5.12) for $\alpha = 1$, $\beta = 0.25$, $L_\xi = L_\eta = 20$, and $\alpha_+ = 1$. Symmetries: $|a_+|^2(\xi, L_\eta/2 - \eta) = |a_+|^2(\xi, L_\eta/2 + \eta)$ and $|a_-|^2(\xi, L_\eta/2 - \eta) = |a_-|^2(\xi, L_\eta/2 + \eta)$ (i.e $|a_+|^2$ $|a_-|^2$ are symmetric with respect to $\eta = L_\eta/2$) and $|b_+|^2(\xi, L_\eta/2 - \eta) = |b_-|^2(\xi, L_\eta/2 + \eta)$ hold as expected.

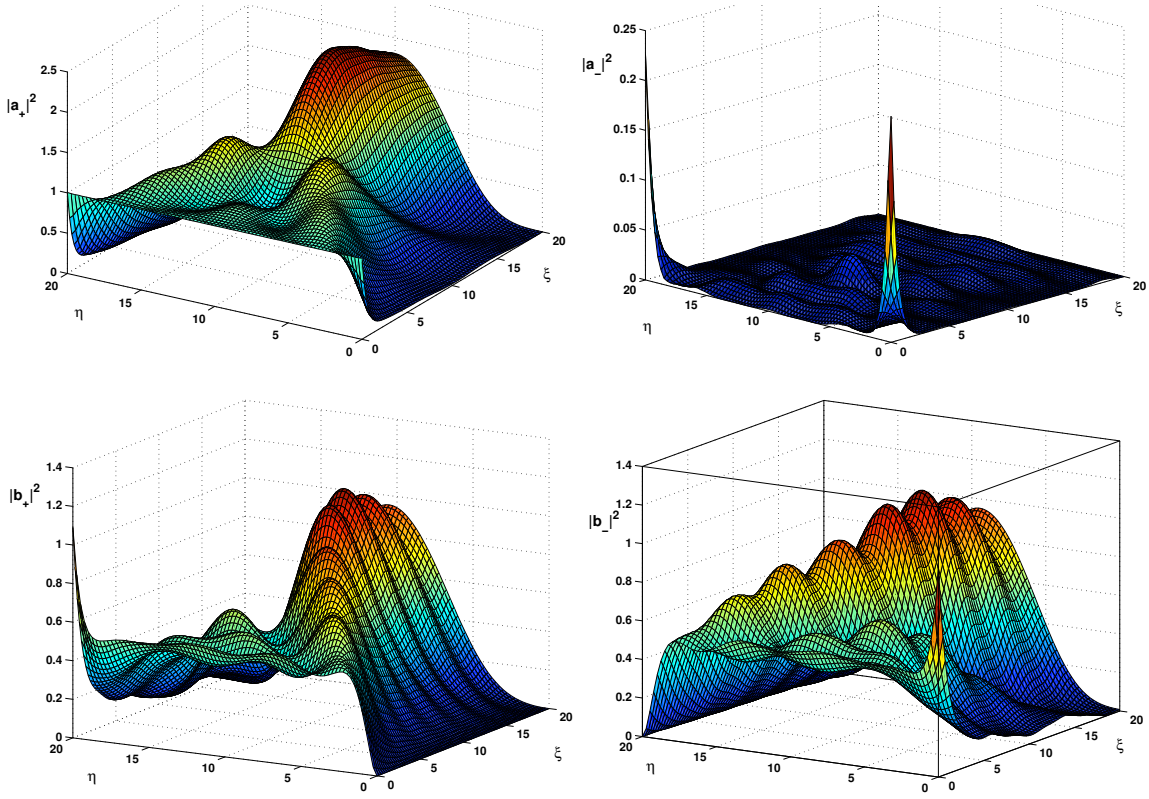

Figure 5.5: Solution surfaces $|a_{\pm}|^2(\xi,\eta)$ and $|b_{\pm}|^2(\xi,\eta)$ on the domain (5.12) for $\alpha = 1$, $\beta = 0.75$, $L_\xi = L_\eta = 20$, and $\alpha_+ = 1$. Symmetries: $|a_+|^2(\xi, L_\eta/2 - \eta) = |a_+|^2(\xi, L_\eta/2 + \eta)$ and $|a_-|^2(\xi, L_\eta/2 - \eta) = |a_-|^2(\xi, L_\eta/2 + \eta)$ (i.e $|a_+|^2$ $|a_-|^2$ are symmetric with respect to $\eta = L_\eta/2$) and $|b_+|^2(\xi, L_\eta/2 - \eta) = |b_-|^2(\xi, L_\eta/2 + \eta)$ hold as expected.

5.3 Transmission of two oblique waves

The stationary transmission of two oblique waves in the coupled-mode equations (3.20)–(3.21) becomes diagonal in the characteristic coordinates (ξ, η):

$$\begin{aligned} \xi &= \frac{\sqrt{p^2+q^2}}{2(pm-nq)}\left((q+2m)X-(p+2n)Y\right), \\ \eta &= \frac{\sqrt{p^2+q^2}}{2(pm-nq)}\left(-qX+pY\right). \end{aligned}$$

After the separation of variables (4.1), the linear coupled-mode equations (3.20)–(3.21) reduce to the PDE system:

$$i\frac{\partial a_1}{\partial \xi} + \Omega a_1 + \alpha a_2 = 0, \tag{5.48}$$

$$i\frac{\partial a_2}{\partial \eta} + \alpha a_1 + \Omega a_2 = 0. \tag{5.49}$$

The coordinate lines $\xi = \xi_0$ are parallel to the wave vector $\mathbf{k}_2 = \mathbf{k}_{\rm out}^{(n,m,0)}$, while the coordinate lines $\eta = \eta_0$ are parallel to the wave vector $\mathbf{k}_1 = \mathbf{k}_{\rm in}$. The problem (5.48)–(5.49) is defined in a bounded domain on the plane (ξ, η). We consider the same rectangle $\mathcal{D}$, defined by (5.12). When the incident wave is illuminated in the wave $\mathbf{k}_1$ but not in the wave $\mathbf{k}_2$, the linear system (5.48)–(5.49) is completed by the boundary conditions:

$$a_1(0,\eta) = \alpha_1(\eta), \qquad a_2(\xi, 0) = 0. \tag{5.50}$$

The boundary value problem of type (5.48)–(5.50) is referred to as Goursat problem or characteristic Cauchy problem in the terminology of [CH]. The linear dispersion relation $\Omega = \Omega(K_\xi, K_\eta)$, where (K_ξ, K_η) are Fourier wave numbers, is given explicitly as

$$\left(\Omega - \frac{K_\xi + K_\eta}{2}\right)^2 = \alpha^2 + \left(\frac{K_\xi - K_\eta}{2}\right)^2. \tag{5.51}$$

Two surfaces of the dispersion relation (5.51) correspond to the two oblique resonant waves. Although the stop band is not the band gap in the characteristic coordinates (ξ, η) , there exist the reference frame on the plane (ξ, η) that moves with constant velocity in time T, such that $K_\xi + K_\xi = const$, where exists a stop band in the dispersion relation (5.51). We set $\Omega = 0$, and write the formal solution of the system (5.48)–(5.49) as follows:

$$\begin{aligned} a_1(\xi,\eta) &= i\alpha \int_0^\xi a_2(\xi,\eta)\, d\xi + a_1(0,\eta) \\ a_2(\xi,\eta) &= i\alpha \int_0^\eta a_1(\xi,\eta)\, d\eta \end{aligned}$$

Interchanging integrals, we reduce the system to the Volterra type integral equation

$$a_1(\xi,\eta) = -\alpha^2 \int_0^\xi \int_0^\eta a_1(\xi,\eta)\, d\eta\, d\xi + a_1(0,\eta)$$

Hence the solution $a_1(\xi,\eta), a_2(\xi,\eta)$ exist and unique. We consider solutions of the system (5.48)–(5.49) at $\Omega = 0$ by using the Fourier transform:

$$a_1(\xi,\eta) = \int_{-\infty}^{\infty} kc(k) e^{i\alpha(k^{-1}\xi + k\eta)} dk, \tag{5.52}$$

$$a_2(\xi,\eta) = \int_{-\infty}^{\infty} c(k) e^{i\alpha(k^{-1}\xi + k\eta)} dk. \tag{5.53}$$

It follows from the boundary conditions (5.50) that

$$kc(k) = \frac{\alpha}{2\pi} \int_0^{L_\eta} \alpha_1(\eta) e^{-i\alpha k\eta} d\eta, \qquad k \in \mathbb{R} \tag{5.54}$$

and

$$0 = \int_{-\infty}^{\infty} c(k) e^{i\alpha k^{-1}\xi} dk, \qquad 0 \le \xi \le L_\xi. \tag{5.55}$$

Interchanging integrals, we reduce the constraint (5.55) to the form:

$$0 = \frac{\alpha}{2\pi i} \int_0^{L_\eta} \alpha_1(\eta) \left(\int_{-\infty}^{\infty} \frac{\sin \alpha(k\eta - k^{-1}\xi)}{k} dk \right) d\eta, \qquad 0 \le \xi \le L_\xi.$$

The inner integral is zero for $\xi > 0$ and $\eta > 0$, due to the table integral 3.871 on p. 474 of [GR]. Therefore, the constraint (5.55) is satisfied and a unique solution of the problem (5.48)–(5.50) exists in the form (5.52)–(5.54).

We illustrate the Fourier transform solution (5.52)–(5.53) with the constant input function:

$$\alpha_1(\eta) = \alpha_1, \qquad \eta \in [0, L_\eta],$$

when $c(k)$ can be found from (5.54):

$$c(k) = \frac{\alpha_1}{2\pi i} \frac{1 - e^{-i\alpha k L_\eta}}{k^2}, \qquad k \in \mathbb{R}.$$

Evaluating Fourier integrals (5.52)–(5.53) with the help of the table integral 3.871 on p. 474 of [GR], we find the explicit solution of the stationary problem:

$$a_1(\xi, \eta) = \alpha_1 J_0(2\alpha\sqrt{\xi\eta}), \qquad a_2(\xi, \eta) = \frac{i\alpha_1\sqrt{\eta}}{\sqrt{\xi}} J_1(2\alpha\sqrt{\xi\eta}), \tag{5.56}$$

where $J_{0,1}(z)$ are Bessel functions [GR]. Figure 6 shows the solution surfaces $|a_1(\xi, \eta)|^2$ and $|a_2(\xi, \eta)|^2$ in the domain (5.12) for $\alpha = 1$, $L_\xi = L_\eta = 10$, and $\alpha_1 = 1$. The integral invariants for the stationary transmission follow from integration of the balance equation:

$$\frac{\partial}{\partial\xi}|a_1|^2 + \frac{\partial}{\partial\eta}|a_2|^2 = 0. \tag{5.57}$$

We define the incident ($\mathcal{I}_{\text{in}}$), transmitted ($\mathcal{I}_{\text{out}}$), and diffracted ($\mathcal{I}_{\text{dif}}$) intensities by

$$\mathcal{I}_{\text{in}} = \int_0^{L_\eta} |a_1(0, \eta)|^2 d\eta, \quad \mathcal{I}_{\text{out}} = \int_0^{L_\eta} |a_1(L_\xi, \eta)|^2 d\eta, \quad \mathcal{I}_{\text{dif}} = \int_0^{L_\xi} |a_2(\xi, L_\eta)|^2 d\xi.$$

The transmittance (T) and diffractance (D) are defined by the same relations (5.2) and the balance identity $T + D = 1$ follows from integration of the balance equation (5.57). The numerical values for T and D are found from numerical integration of

the solution surfaces (5.58) as follows:

$$T \approx 0.032, \qquad D \approx 0.968,$$

such that $T + D \approx 1$. These values show that the incident wave is diffracted to the oblique resonance wave, such that only 3.2% of the wave energy remains in the transmitted wave.

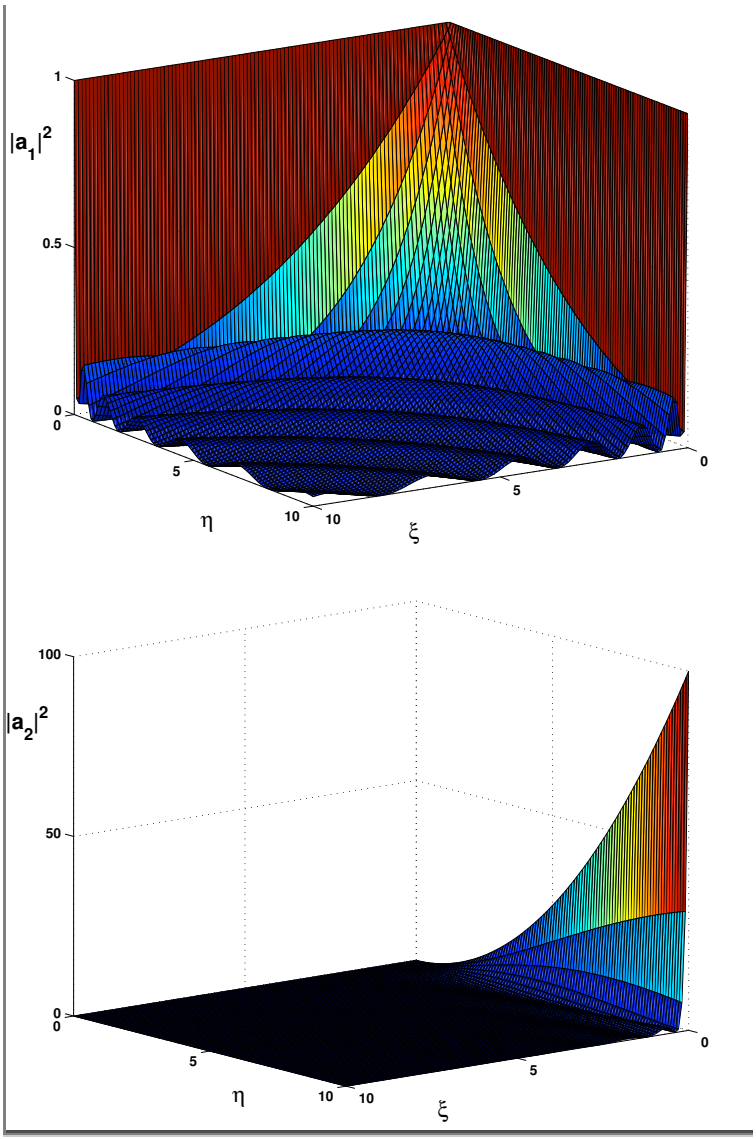

Figure 5.6: Solution surfaces $|a_1|^2(\xi, \eta)$ and $|a_2|^2(\xi, \eta)$ on the domain (5.12) for $\alpha = 1$, $L_\xi = L_\eta = 10$, and $\alpha_1 = 1$.

Chapter 6

Summary and open problems

We have shown that the coupled-mode equations can be used for analysis and modeling of resonant interaction of Bloch waves in low-contrast cubic-lattice three-dimensional photonic crystals.

We have proved existence and uniqueness of solution for the N-wave coupled-mode system boundary value problem in any convex domain for a linear and non-linear cases.

The analytical solutions for the linear stationary transmission problem are found by using separation of variables and generalized Fourier series.

Non-stationary transmission problems are also of interest, and very few analytical results are available on local and global well-posedness of the non-stationary nonlinear coupled-mode equations.

Finally, numerical integration of the coupled-mode equations using multi-symplecticity seems to be very promising.

Bibliography

[AP] D. Agueev and D. Pelinovsky [2004] Wave resonances in low-contrast photonic crystals. *SIAM J. Appl. Math.*, to be published.

[AS] A. Arraf and C.M. de Sterke [1998] Coupled-mode equations for quadratically nonlinear deep gratings, *Phys. Rev. E* **58**, 7951–7958.

[AJ1] N. Akozbek and S. John [1998] Optical solitary waves in two- and three-dimensional nonlinear photonic band-gap structures, *Phys. Rev. E* **57**, 2287–2319.

[AJ2] N. Akozbek and S. John [1998] Self-induced transparency solitary waves in a doped nonlinear photonic band gap materials, *Phys. Rev. E* **58**, 3876–3895.

[BF1] A. Babin and A. Figotin [2001] Nonlinear photonic crystals: I. Quadratic nonlinearity, *Waves in Random Media* **11**, R31–R102.

[BF2] A. Babin and A. Figotin [2002] Nonlinear photonic crystals: II. Interaction classification for quadratic nonlinearities, *Waves in Random Media* **12**, R25–R52.

[BS] N. Bhat and J.E. Sipe [2001] Optical pulse propagation in nonlinear photonic crystals, *Phys. Rev. E* **64**, 056604

[Br] T. J. Bridges [1997] Multi-symplectic structures and wave propagation. *Math. Proc. Camb. Phil. Soc.* **121**, 147–190.

[BR] T. J. Bridges and S. Reich [2001] Multi-symplectic integrators: numerical schemes for Hamiltonian PDEs that conserve symplecticity. *Phys. Lett. A* **284**, 184–193.

[CL] E.A. Coddington and N. Levinson, *Theory of Ordinary Differential Equations*, (McGraw-Hill, New York, 1955).

[CH] R. Courant and D. Hilbert [1962] *Methods of Mathematical Physics.* Interscience Publisher.

[E] M. S. P. Eastham [1973] *The Spectral Theory of Periodic Differential Equations.* Scottish Acad. Press, Edinburgh, London.

[FK1] A. Figotin and P. Kuchment [1994] Band-gap structure of the spectrum of periodic and acoustic media. I. Scalar model. *SIAM J. Appl. Math.* **56**, 68–88.

[FK2] A. Figotin and P. Kuchment [1994] Band-gap structure of the spectrum of periodic and acoustic media. II. Two-dimensional photonic crystals. *SIAM J. Appl. Math.* **56**, 1561–1620.

[GWH] R.H. Goodman, M.I. Weinstein, and P.J. Holmes [2001] "Nonlinear propagation of light in one-dimensional periodic structures", *J. Nonlin. Science* **11**, 123–168.

[GR] I.S. Gradshtein, I.M. Ryzhik [2000] *Table of integrals, series, and products* Academic Press.

[JMW] J. Joannopoulos, M. Meade, and J. Winn [1995] *Photonic Crystals: Molding the Flow of Light.* Princeton University Press.

[Ki] C. Kittel [1996] *Introduction to Solid–State Physics* John Wiley & Sons.

[KF] A. N. Kolmogorov and S. V. Fomin [1970] *Introductory Real Analysis.* Prentice-Hall.

[Ko] Adrian Korpel [1988] *Acousto-Optics.* Marcel Dekker, Inc.

[K1] P.Kuchment [1993] *Floquet Theory for Partial Differential Operators* Birkhauser, Basel.

[K2] P. Kuchment [1999] The mathematics of photonic crystals, *Mathematical Modeling in Optical Sciences* SIAM, Philadelphia.

[LL1] L. D. Landau and E. M. Lifshitz [1971] *The Classical Theory of Fields.* Pergamon Press.

[LL2] L. D. Landau E. M. Lifshitz [1984] *Electromagnetics of Continuos Media.* Pergamon.

[MPS] J. Marsden, G. Patric and S. Shkoller [1998] Multisymplectic geometry, variational integrators, and nonlinear PDEs. *Comm. Math. Phys.,* **199**, 351–391.

[O] P. J. Olver [1986] *Application of Lie Groups to Differential Equations.* Springer-Verlag: New York.

[PSBS] D. Pelinovsky, J. Sears, L. Brzozowski, and E.H. Sargent [2002] Stable all-optical limiting in nonlinear periodic structures. I: Analysis, *J. Opt. Soc. Am. B* **19**, 43–53.

[PS] D.E. Pelinovsky and A. Scheel [2003] Spectral analysis of stationary light transmission in nonlinear photonic structures, *J. Nonlin. Science,* **13**, 347-396.

[RS] M. Reed and B. Simon [1978] *Methods of Modern Mathematical Physics, Vol. IV: Analysis of Operators.* Academic Press, New York.

[S] R. Syms [1986] Path-integral formulation of multiple scattering problems in integrated optics. *Appl. Opt.* **25**, 4402–4412.

[SU] G. Schneider and H. Uecker [2003] Existence and stability of modulating pulse solutions in Maxwell's equations describing nonlinear optics, *Z. angew. Math. Phys.* **54**, 677–712.

[SGS] J.L. Sheriff, I.A. Goldthorpe, and E.H. Sargent [2004] Optical limiting and intensity-dependent diffraction from low-contrast nonlinear periodic media: coupled-mode analysis, *Phys. Rev. E* , to be published.

[Sh] J.L. Sheriff [2003] Coupled-mode theory in low-contrast nonlinear photonic crystals, *B.Sc. thesis, University of Toronto*

[SS1] C.M. de Sterke and J.E. Sipe [1998] Envelope-function approach for the electrodynamics of nonlinear periodic structures, *Phys. Rev. A* **38**, 5149–5165.

[SS2] C.M. de Sterke and J.E. Sipe [1989] Extensions and generalizations of an envelope-function approach for the electrodynamics of nonlinear periodic structures, *Phys. Rev. A* **39**, 5163–5178.

[SSS] C.M. de Sterke, D.G. Salinas, and J.E. Sipe [1996] Coupled-mode theory for light propagation through deep nonlinear gratings, *Phys. Rev. E* **54**, 1969–1989.

[SS] C.M. de Sterke and J.E. Sipe [1994] Gap solitons, *Progress in Optics* , **33**, 203.

[St] W. Strauss [1992] *Partial Differential Equations: an Introduction* , Wiley & Sons, New York.